geosciences

MDPI

Review

Metamorphic Remnants of the Variscan Orogeny across the Alps and Their Tectonic Significance

Manuel Roda [1,*], Maria Iole Spalla [1], Marco Filippi [1], Jean-Marc Lardeaux [2,3], Gisella Rebay [4], Alessandro Regorda [1], Davide Zanoni [1], Michele Zucali [1] and Guido Gosso [1]

[1] Dipartimento di Scienze della Terra, Università degli Studi di Milano, Via Mangiagalli 34, 20133 Milano, Italy; iole.spalla@unimi.it (M.I.S.); marco.filippi@unimi.it (M.F.); alessandro.regorda@protonmail.ch (A.R.); davide.zanoni@unimi.it (D.Z.); michele.zucali@unimi.it (M.Z.); guido.gosso@unimi.it (G.G.)
[2] UMR Geoazur, Université Nice Sophia-Antipolis, 250 Rue A. Einstein, 06560 Valbonne, France; lardeaux@wanadoo.fr
[3] Center for Lithospheric Research, Czech Geological Survey, 11821 Praha, Czech Republic
[4] Dipartimento di Scienze della Terra e dell'Ambiente, Università degli Studi di Pavia, Via Ferrata 1, 27100 Pavia, Italy; gisella.rebay@unipv.it
* Correspondence: manuel.roda@unimi.it

Abstract: Lithospheric slices preserving pre-Alpine metamorphic imprints are widely described in the Alps. The Variscan parageneses recorded in continental, oceanic, and mantle rocks suggest a heterogeneous metamorphic evolution across the Alpine domains. In this contribution, we collect quantitative metamorphic imprints and ages of samples that document Variscan tectonometamorphic evolution from 420 to 290 Ma. Based on age distribution and metamorphic imprint, three main stages can be identified for the Variscan evolution of the Alpine region: Devonian (early Variscan), late Devonian–late Carboniferous (middle Variscan), and late Carboniferous–early Permian (late Variscan). The dominant metamorphic imprint during Devonian times was recorded under eclogite and HP granulite facies conditions in the Helvetic–Dauphinois–Provençal, Penninic, and eastern Austroalpine domains and under Ep-amphibolite facies conditions in the Southalpine domain. These metamorphic conditions correspond to a mean Franciscan-type metamorphic field gradient. During the late Devonian–late Carboniferous period, in the Helvetic–Dauphinois–Provençal and central Austroalpine domains, the dominant metamorphic imprint developed under eclogite and HP granulite facies conditions with a Franciscan field gradient. Amphibolite facies conditions dominated in the Penninic and Southalpine domains and corresponded to a Barrovian-type metamorphic field gradient. At the Carboniferous–Permian transition, the metamorphic imprints mainly developed under amphibolite-LP granulite facies conditions in all domains of the Alps, corresponding to a mean metamorphic field gradient at the transition between Barrovian and Abukuma (Buchan) types. This distribution of the metamorphic imprints suggests a pre-Alpine burial of oceanic and continental crust underneath a continental upper plate, in a scenario of single or multiple oceanic subductions preceding the continental collision. Both scenarios are discussed and revised considering the consistency of collected data and a comparison with numerical models. Finally, the distribution of Devonian to Triassic geothermal gradients agrees with a sequence of events that starts with subduction, continues with continental collision, and ends with the continental thinning announcing the Jurassic oceanization.

Keywords: metamorphic field gradients; subduction; collision; Pangea breakup; Variscan tectonometamorphic evolution

Citation: Roda, M.; Spalla, M.I.; Filippi, M.; Lardeaux, J.-M.; Rebay, G.; Regorda, A.; Zanoni, D.; Zucali, M.; Gosso, G. Metamorphic Remnants of the Variscan Orogeny across the Alps and Their Tectonic Significance. *Geosciences* **2023**, *13*, 300. https://doi.org/10.3390/geosciences13100300

Academic Editors: Jesus Martinez-Frias and Olivier Lacombe

Received: 13 July 2023
Revised: 16 September 2023
Accepted: 2 October 2023
Published: 6 October 2023

1. Introduction

The Variscan belt constitutes the skeleton of the European continental crust and, for this reason, is one of the most investigated orogens in the world. The palaeogeographic-geodynamic reconstructions are numerous and contrasted, and the proposed subdivisions

into structural domains (e.g., [1–20]) are rendered incomplete by the Meso–Cenozoic "tectonic disturbance" induced by the Betic Cordillera, the Pyrenees, and the Alps (Figure 1). The resolution of the Variscan structural setting of these domains would allow for correlating the central and the southern part of the European Variscides, possibly solving doubts or helping to overcome misfits. In particular, numerous palaeogeographic-tectonic interpretations have recently been proposed for the Alps, generally based on the lithostratigraphic affinity between lithotectonic units constituting the pre-Alpine continental crust of the chain [21–28]. However, the validity of these reconstructions becomes critical when they are also proposed for the axial zone of the Alps where, differently from the external structural domains, the tectonic reworking was pervasive during the Alpine convergence. In present-day subduction settings [29–31], tectonic erosion is one of the main destructive mechanisms that characterize such systems. It implies a significant reorganization of the original structure of the upper plate margins and strongly contributes to the generation of the tectonic mélange that typically characterizes subduction complexes [32]. The latter generally coincide with the axial zones of the orogens, so early remarked by [33] as places in which there are "portions of terrains that are not in their place, lying on an accidental substrate, which is not their original substrate". In this context, it appears more productive to examine the Variscan metamorphic imprints recorded across internal and external domains of the Alps, which, albeit with a discontinuous record, indicate the potential existence of one or more suture zones, as already attempted for exploring the possible pre-Alpine evolution of the Palaeozoic continental crust with quantitative geodynamic modelling (e.g., [34,35]).

In this light, this contribution shows the distribution of quantitative Variscan metamorphic conditions and the compositional affinity of protoliths across the different structural domains of the Alps. This information will be completed with the age relative to the different Variscan metamorphic imprints that range from Devonian to early Permian. In the end, the Variscan metamorphic signatures and their ages are here discussed in relation to the metamorphic gradients that have largely been used to interpret subduction-collision chains [36–44]. Therefore, rather than identifying and unravelling the palaeogeographical origin of lithotectonic units, this study aims at the identification of the link beyond the "Meso-Cenozoic disturbances", to find relationships between the Variscan subduction-collision metamorphic markers and their distribution across the Alpine suture.

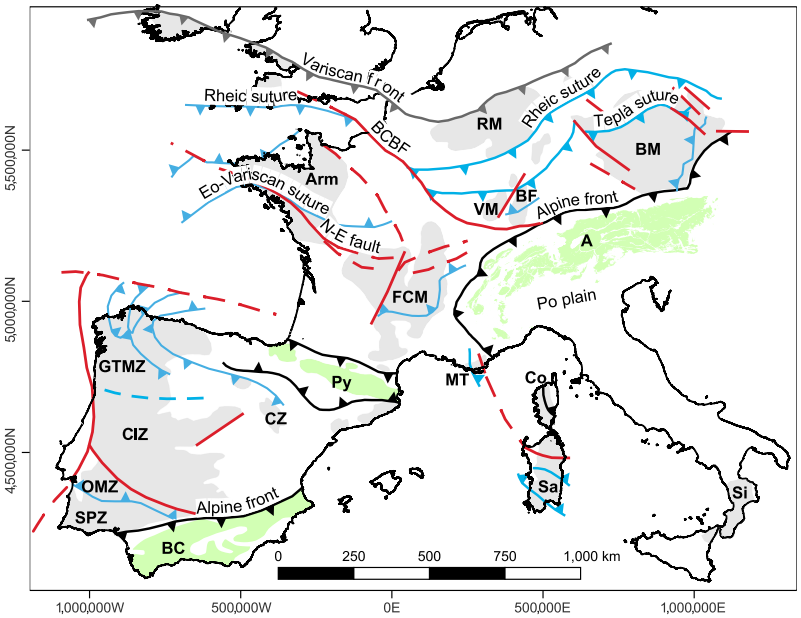

Figure 1. Simplified tectonic sketch of the Variscan belt (modified after [15,35]). Grey areas contour the Variscan massifs and green areas contour the Pyrenees, Betic Cordillera, and the Alps. Grey and

black lines show Variscan and Alpine fronts, respectively. Blue lines show Variscan sutures and red lines show main Variscan faults. A—Alps; Arm—Armorican Massif; BC—Betic Cordillera; BCBF—Bristol Channel–Bray Fault; BF—Black Forest; BM—Bohemian Massif; CZ—Cantabrian Zone; CIZ—Central Iberian Zone; Co—Corsica; FCM—French Central Massif; GTMZ—Galicia-Trás-os-Montes Zone; MT—Maures-Tanneron Massif; OMZ—Ossa Morena Zone; Py—Pyrenees; Sa—Sardinia; RM—Rhenish Massif; Si—Sicilian-Apulian basements; SPZ—South Portuguese Zone; VM—Vosges Massif. Coordinate system WGS 84, UTM Zone 32N.

2. Geological Setting

The Alps were generated by the subduction of the Ligurian-Piedmont ocean (Western Tethys) under the Adria continental margin during the Meso–Cenozoic time, followed by the collision of the European passive continental margin. The chain suture stretches from Graz in SE Wien to the Gulf of Genova in NW Italy, south of which it is truncated by the Neogenic Algero-Provençal basin (Figure 2). At its eastern end, it disappears under the Neogene sedimentary rocks of the Pannonian basin system, which separates the Alps from the Carpathians [45–48].

Along a western section from the Alpine front to the Po plain (Figure 2), the main structural domains are (e.g., [49–51]) (a) the European foreland basin, underthrusted by the Alpine belt during the final stages of convergence; (b) the pre-Alpine basement and cover of the Helvetic–Dauphinois–Provençal domain, affected by the inversion of Mesozoic listric faults into a thrust system during Palaeogene Alpine continental collision; (c) the subduction system, between the Penninic Front (PF) and the Periadriatic Fault System (PFS), which is constituted of a mélange of Penninic and Austroalpine continental nappes wrapped by oceanic covers and basement rocks, belonging to the sutured western Tethys ocean; and (d) the Southalpine domain that consists of continental basements and cover units only locally affected by low-grade Alpine metamorphism and involved in a south-verging thrust system active since the Cretaceous period (e.g., [52–54]). This domain constitutes the hinterland of the Alpine belt.

The study of the tectonic setting of the area was integrated via the ECORS-CROP-NFP20-TRANSALP seismic project [55], which identified the subduction complex within the axial part of the chain. Such a hidden structure consists of a Cretaceous–Palaeogene rootless crustal prism, which is confined by the PF towards the Helvetic–Dauphinois–Provençal domain and by the PFS towards the Southalpine domain. The rootless crustal prism records Cretaceous to Palaeogene high-pressure and ultra-high-pressure metamorphism (e.g., [16,56–58]) and includes continental rocks that were buried in the subduction system through either continental collision or ablative subduction. In the second case, the high-pressure and ultra-high-pressure continental rocks were ablated from the upper continental plate by the subducting oceanic plate before continental collision (e.g., [49,56,59,60]). Consequently, regardless of the chosen interpretation, it clearly appears that in the subduction complex, the possibility of individuating a continuity of pre-Alpine structures and lithostratigraphy, which allows for the reconstruction of Variscan lithotectonic units, is strongly compromised.

Since Variscan metamorphic relicts were found in the pre-Alpine Penninic and Austroalpine continental crust, it is possible to compare their metamorphic imprints with those of the basement rocks of the Helvetic–Dauphinois–Provençal and Southalpine domains, where Alpine tectonics has been less destructive [22,25,34,61,62], and potentially identify scars of the Variscan suture.

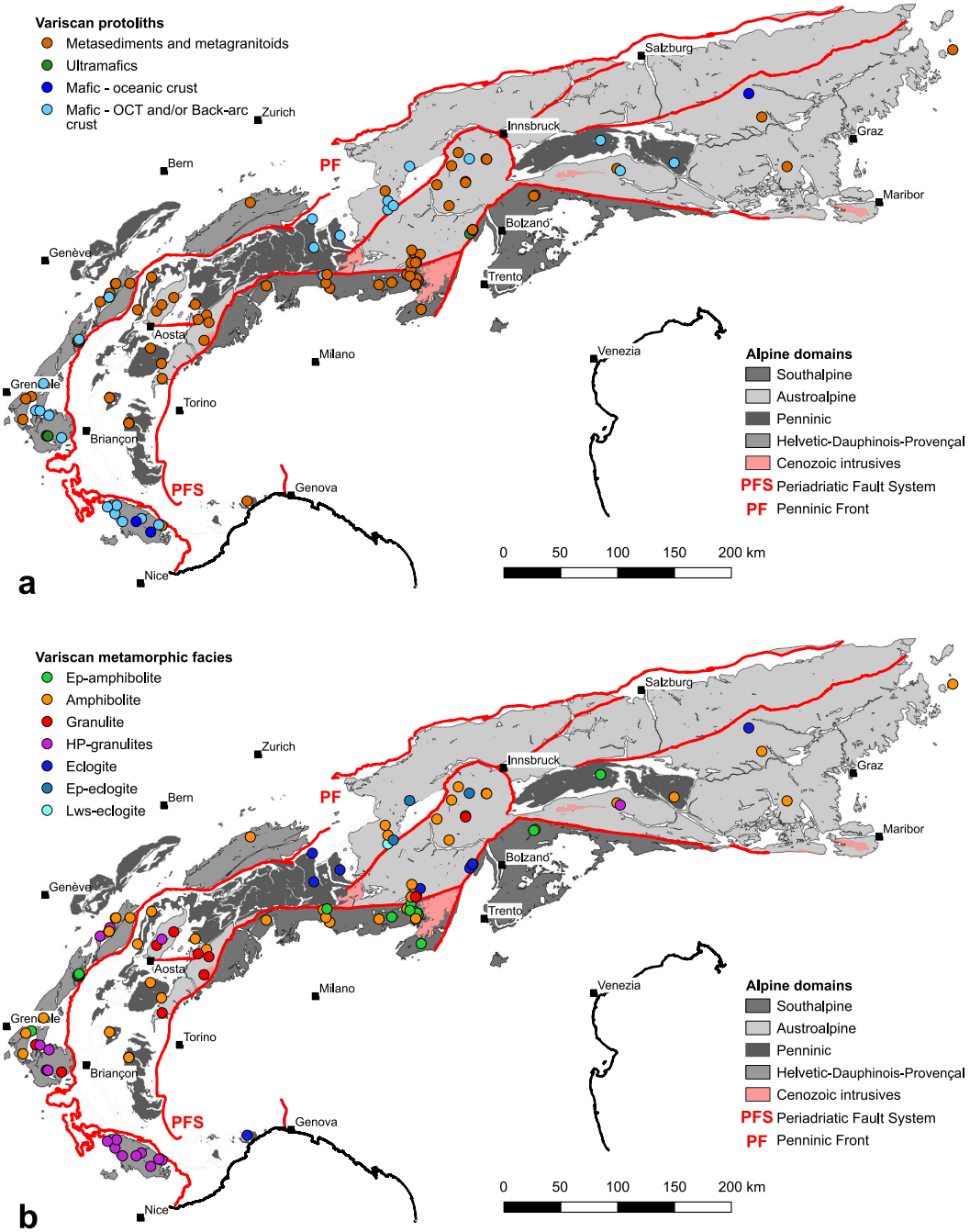

Figure 2. (**a**) Variscan protolith and rock types. (**b**) Variscan metamorphic imprints. See tectonic unit, location, and reference coding in Appendix A

3. Rock Types and Metamorphic Imprints

In this section, we describe the rock types from the different domains of the Alps (Southalpine, Austroalpine, Penninic, and Helvetic–Dauphinois–Provençal; Figure 2) that display evidence of Variscan metamorphism over a time frame spanning from early Devonian to early Permian (ca. 420 to 290 Ma; [63]). Data on each rock, including tectonic unit, location, interpreted protolith affinity (continental, oceanic, mantle, or undefined crusts), mineral assemblage, temperature and pressure conditions, and the age of the Variscan metamorphic imprint, are reported in Tables 1–4, following the different structural domains. The different rock types mainly consist of metasediments or metagranitoids of continental affinity in all domains, although metabasites of oceanic affinity and mantle rocks are also reported in the Austroalpine, Penninic, and Helvetic–

Dauphinois–Provençal domains (Figure 2a). The first letter of the sample code in the tables is the domain (S = Southalpine, A = Austroalpine, P = Penninic, and H = Helvetic–Dauphinois–Provençal), and the second is the age (v = Variscan, p = Permian).

3.1. Southalpine Domain

The Southalpine domain represents a well-preserved portion of the pre-Alpine Adria crust, minimally affected by the Alpine metamorphism during the development of an E-W-trending and S-verging fold and thrust system and involving the pre-Alpine basement and Permian–Mesozoic volcanic and sedimentary sequences [52–54,64–73]. The basement rocks (labelled Sv in Table 1) are exposed from the eastern termination of the Southalpine thrust system to the Canavese Line (the westernmost portion of the Periadriatic Fault System).

The Variscan metamorphic rocks of the Southalpine basement include micaschists, paragneisses, metagranitoids, metabasites, quartzites, carbonatic schists, marbles, and pegmatites. The dominant metamorphic imprints (Figures 2b and 3a,b) were quantitatively inferred mainly from metapelites and their ages generally fall between 330 and 340 Ma except for two younger ages in the Ivrea and Dervio–Olgiasca Zones [74,75]. In these rocks, cm sized relicts preserve mineral assemblages of low-temperature and intermediate-pressure conditions (epidote-amphibolite facies imprints; Figures 2b and 3a), recorded during the T-prograde Variscan evolutions and predating the T_{max} imprint (ca. 385 Ma; [76–81]. The late Carboniferous syn-metamorphic structures consist of a regional scale fold system, generally associated with an axial plane foliation marked by greenschist facies minerals, locally mylonitic ([61] and refs therein). The microstructural and petrologic analyses of metamorphic pebbles from the late orogenic–early Permian conglomerates, capping the central Southalpine basement, reveal that coherent metamorphic evolutions were recorded via Variscan rocks, exposed to erosion during early Permian times [80,82,83]. Towards the western termination of the Southalpine basement, a continuous horizon of metabasites, minor paragneisses, metagabbros, retrogressed eclogites, and lenses of ultramafites are comprised in the Serie dei Laghi Complex. Here, the dominant metamorphic imprint under amphibolite facies conditions was dated between 307 and 359 Ma (e.g., [84,85]). This horizon separates two main units of the Serie dei Laghi Complex (Strona-Ceneri and Scisti dei Laghi), and it is interpreted as ophiolitic relicts marking a pre-Variscan suture, successively deformed and re-equilibrated under amphibolite facies conditions together with the surrounding rocks (e.g., [86,87]). The west-ending portion of the Southalpine basement, separated from the subduction complex by the Periadriatic Fault System, corresponds to the Ivrea Zone where the dominant metamorphic imprint in granulite facies is late to post-Variscan (i.e., Permian; [62,74]). Conversely, the eastern sector of the Southalpine basement is mainly constituted of metapelites and metapsammites with intercalations of acidic and basic metavolcanics ([88] and refs therein). In contrast with the central and western Southalpine basement, the dominant metamorphic imprint never exceeds the epidote amphibolite to greenschists facies conditions (Figure 2b), with metamorphic ages comprised between Devonian and Carboniferous. Starting from the Cadore region in the eastern Alps, the Variscan basement consists of non- to low-grade metamorphic sequences of the eastern Palaeocarnic chain [89].

3.2. Austroalpine Domain

The metamorphic basement of the Austroalpine domain is generally referred to the Adriatic margin (e.g., [49]) and is interpreted as belonging to Gondwana before being involved in the Variscan collision [28,90,91]. In the western Austroalpine domain, the Variscan metamorphic imprint is generally preserved in structural relicts, whereas it is better preserved in the central and eastern parts. Here, eclogites and related high-pressure rocks have been detected in metabasite lenses, which are enclosed in high- to medium-grade metapelites. They generally show a polyphasic tectonometamorphic evolution [35,88,92–98], and their radiometric ages range between early Devonian and Carboniferous (Table 2). High-pressure rocks mainly occur in the Schobergruppe, Oetztal–Stubai, Silvretta, and Languard-Campo

nappes (Figure 2). Here, Variscan high-pressure assemblages developed both in mafic and acidic igneous protoliths and in metasediments are variably re-equilibrated mainly under amphibolite facies conditions (Figure 2, [35,61]), and this attests the deep subduction of the continental lithosphere. Eclogite protoliths from Silvretta are of MORB type and have mainly Mississippian metamorphic ages [99]. Variscan eclogitized mantle rocks from the Austroalpine domain (Nonsberg–Ulten Zone) consist of spinel lherzolite evolving to garnet peridotite (Figure 3d), and the inferred pressure prograde path indicates cooling during deep burial in the subduction system [94,96,100–102].

3.3. Penninic Domain

The continental crust belonging to the Penninic domain consists of Precambrian to early Palaeozoic polymetamorphic or monometamorphic basement [90,91,103,104] comprising mafic and acidic metaintrusives and metasediments (labelled Pv in Table 3 and Figure 2a). In greater detail, Variscan metamorphic rocks consist of high-grade paragneisses with minor marbles, metagranitoids, and metabasites [105–107]. In the Grand St. Bernard nappe garnet-bearing amphibolites, locally preserving eclogite facies mineral assemblages [91,103,108] occur within garnet-, staurolite-, and aluminum silicate-bearing metapelites [103,104,109–112]. High-pressure rocks and eclogites also occur in the mafic lenses of the polymetamorphic basement of Savona Massif (Figure 3e,f; western Alps), of the Adula and Suretta nappes (central Alps), and of the Tauern Window (eastern Alps) [113–122]. The Variscan dominant metamorphic imprint generally developed under eclogite or amphibolite facies conditions (Figure 2b). Geochronologic determinations point to early Devonian ages in the Savona Massif, Tauern Window, and Adula Variscan basements and to early Carboniferous in the other Penninic nappes of the western and central Alps (Table 3 and refs therein).

3.4. Helvetic–Dauphinois–Provençal Domain

The Helvetic–Dauphinois–Provençal domain, which derives from the pre-Alpine European passive margin (the lower plate of the Alpine subduction), has only been involved in the Alpine convergent system since the continental collision, and as a result, it has largely avoided most of the structural and metamorphic effects caused by subduction. The metamorphic pre-Alpine basement (labelled Hv in Table 4) is found in the "External Crystalline Massifs" (Argentera, Pelvoux–Belledonne–Grandes Rousses, Mont Blanc–Aiguilles Rouges, and Aar-Gotthard), where pre-Alpine structural and metamorphic features are well preserved (e.g., [23,24,48,106,123–127]). The "External Crystalline Massifs", exposed in the western Alps, consist of metamorphic rocks with ages ranging from Cambrian to Carboniferous, capped by late Carboniferous to Permian sedimentary sequences and intruded by Permo–Carboniferous granitoids. All of these rocks show a discontinuous Alpine metamorphic and structural signature (e.g., [24,128–131]). Variscan eclogites, granulites, amphibolites, high-grade metapelites, and metagranitoids [124,126,127,132–138] document a polyphase metamorphic history, ranging from eclogite–granulite to Ep-amphibolite facies (Figure 2b). Eclogites and high-pressure granulites occur as lenses or boudins (Figure 3g) wrapped by sillimanite biotite-bearing foliations within migmatitic gneisses. The rims of these pods are extensively re-equilibrated under amphibolite or granulite facies conditions (Figure 3h). Radiometric ages related to high-pressure imprints are mainly Carboniferous (Table 4), with some old Devonian determinations whose reliability is questioned today [139]. Variscan high-pressure assemblages have never been detected in the Aar-Gotthard Massif, where Variscan imprints developed under amphibolite facies conditions during early Carboniferous times (Table 4). Late Carboniferous to early Permian granitoid stocks and acidic and mafic dykes crosscut the migmatitic foliations and high-pressure pods [130].

In the Permian–Triassic period, a high temperature-low pressure metamorphism and intense mafic to acidic igneous activity affected the Variscan continental crust of the

Penninic, Austroalpine, and Southalpine domains. No similar metamorphic features have been described in the rocks of the Helvetic–Dauphinois–Provençal domain [62,140].

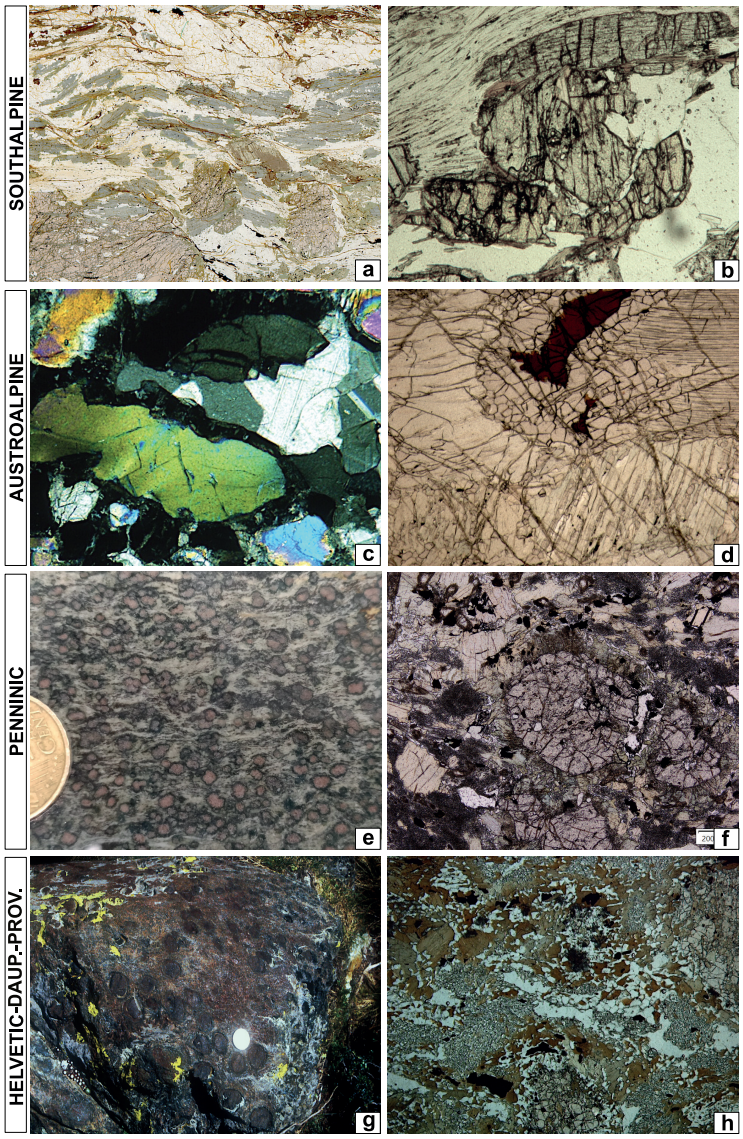

Figure 3. Examples of Variscan rocks from the different Alpine domains. (**a**) Chloritoid, biotite, white mica, and garnet-bearing metapelites from Southalpine basement (eastern Orobic Alps, Upper Val Camonica) indicating an epidote-amphibolite facies metamorphic imprint. SPO of chloritoid marks S1 foliation. Plane-polarized light; long side of the photograph = 1 cm. (**b**) Garnet, white mica, kyanite, staurolite, and biotite-bearing metapelites from upper Como Lake, Southalpine basement, indicating amphibolite facies conditions during S2 development. Plane-polarized light; long side of photograph = 3.5 mm. (**c**) Garnet, scapolite, diopside, and plagioclase syn-D1 granulitic assemblage in metabasites from Austroalpine domain of central Alps (Languard-Campo nappe). Alpine garnet coronas rim granulitic Variscan minerals. Crossed polars; long side of photograph = 0.1 mm. (**d**) Olivine, garnet, and biotite in garnet peridotites of Nonsberg–Ulten Zone. Plane-polarized light; long side of photograph = 2.2 mm. (**e**) Garnet, omphacite, and amphibole in eclogite lenses enclosed in the paragneisses of the Savona Massif. (**f**) Partly re-equilibrated garnet, omphacite, zoisite, and rutile eclogite facies assemblage from Savona Massif. Late kelyphitic amphibole developed at garnet rims. Plane-polarized light; long side of photograph = 1.7 mm (**g**) Eclogite boudin in migmatitic paragneisses of the Argentera Massif with cm sized garnets. (**h**) Retrogressed eclogites with garnet, zoned amphibole, and relict omphacite replaced by diopside–plagioclase symplectite, from the Argetera Massif. Plane-polarized light; long side of photograph = 5 mm.

Table 1. Rock type for the Southalpine domain including the metamorphic assemblages, P-T conditions, and Variscan ages. Cc = continental crust; Oc = oceanic crust; Ma = mantle; Un = undefined crust. Geochronological data acquisition: ⊙ mineral separation. See reference coding in Appendix A. Mineral abbreviations are after [141].

Tect. Unit	Location	Group/Rock	Assemblage	Temp (°C)	Pres (GPa)	Age (Ma)	Method	Refs	Code
Serie dei Laghi Complex	Val Cannobbina	Cc metapelite	Qz, Pl, Grt, St, Bt, Hbl	640 ± 50	0.70 ± 0.1	333 ± 26	Ar/Ar (Wm) ⊙	[84,142]	Svc1
Domaso–Cortafò Zone	Como Lake	Cc metapelite	Grt, Bt, Wm, Cld, Pl, Qz			385	K/Ar (Wm) ⊙	[76,77,143,144]	Svco2a
		amphibolite	Amp, Grt, Pl, Qz, Bt, Ilm						
Domaso–Cortafò Zone	Como Lake	Cc metapelite	St, Grt, Bt, Ms, Qz, Ky	605 ± 45	0.90 ± 0.2	330 ± 8	K/Ar (Amp) ⊙	[77,144–146]	Svco2b
		amphibolite	Amp, Grt, Pl, Qz, Bt, Rt						
Monte Muggio Zone	Monte Muggio	Cc metapelite	Qz, Chl, Bt, St, Ky, Ms	570 ± 10	0.80 ± 0.1	330 ± 10	K/Ar (Amp) ⊙	[83,145–148]	Svc3
Dervio–Olgiasca Zone	Corenno Plinio	Cc metapelite	Ms, Bt, Grt, Pl, Qz, St, Ky	630 ± 30	0.85 ± 0.15	315 ± 3	U/Pb (Mnz) ⊙	[75,144,149]	Svc5a
		amphibolite	Amph, Pl, Qz, Cpx, Bt, Ilm						
Dervio–Olgiasca Zone	Corenno Plinio	Cc metapelite	Ms, Bt, Grt, Pl, Qz, St, Ky	560 ± 30	1.0 ± 0.25	330 ± 10	K/Ar (Wm) ⊙	[144,146,149]	Svc5b
		amphibolite	Grt, Amph, Pl, Qz, Rt						
Val Vedello Basement	Val Vedello	Cc metapelite	Ms, Bt, Grt, Pl, Qz, St, Ky	629 ± 39	0.90 ± 0.2	330 ± 10	K/Ar (Wm) ⊙	[69,82,146]	Svc4
North-Eastern Orobic Basement (A)	Lago Belviso	Cc metapelite	Grt, St, Bt, Ms, Pl, Qz	615 ± 45	1.00 ± 0.15	330 ± 10	K/Ar (Amp) ⊙	[145,150]	Svc6a
North-Eastern Orobic Basement (A)	Lago Belviso	Cc metapelite	Grt, Cld, Bt, Ms, Pl, Qz	500 ± 20	0.85 ± 0.1	Devonian		[76,150]	Svc6b
North-Eastern Orobic Basement (B)	Edolo	Cc metapelite	Chl, Bt, Grt	495 ± 55	0.55 ± 0.2	330 ± 10	K/Ar (Amp) ⊙	[71,82,145]	Svc7
Eastern Orobic Basement	Val Camonica	Cc metapelite	Qz, Pl, Grt, Bt, Wm, Cld, Rt, Ilm	510 ± 60	0.85 ± 0.15	Devonian		[76,81]	Svc14a
Eastern Orobic Basement	Val Camonica	Cc metapelite	Qz, Pl, Grt, Bt, Wm, St, Ilm	600 ± 50	0.55 ± 0.15	330 ± 10	K/Ar (Amp) ⊙	[81,145]	Svc14b
Eastern Orobic Basement	Val Camonica	Cc metapelite	Qz, Pl, Grt, Bt, Wm, St, And, Ep, Ilm	550 ± 30	0.30 ± 0.1	>late Permian		[81]	Svc14c
Trompia Valley Basement	Passo Maniva	Cc metapelite	Grt, Cld, Ms, Pl, Qz	525 ± 25	1.10 ± 0.2	late Devonian		[78–80]	Svc9
Eisacktal	Brixen	Cc metapelite	Qtz, Pl, Bt, Kfs, Grt	625 ± 25	>0.3	Devonian		[151]	Svc10
Eisacktal	Brixen	Cc metapelite	Bt, Crd, Kfs, Pl, Qz, Sil	500 ± 50	0.60 ± 0.05	Carboniferous		[151]	Svc11

Table 2. Rock type for the Austroalpine domain including the metamorphic assemblages, P-T conditions, and Variscan age. Cc = continental crust; Oc = oceanic crust; Ma = mantle; Un = undefined crust. Geochronological data acquisition: ⊙ mineral separation; ⊖ mineral separation and trace elements; ⊘ in situ; ⊕ in situ and trace elements. See reference coding in Appendix A. Mineral abbreviations are after [141].

Tect. Unit	Location	Group	Assemblage	Temp (°C)	Pres (GPa)	Age (Ma)	Method	Refs	Code
Dent Blanche	Valpelline	Cc metapelite	Grt, Bt, Sil	703 ± 42	0.55 ± 0.1	289.1 ± 6.3	U/Pb (Zrn) ⊖	[152–154]	Avc14
Dent Blanche	Valpelline	Cc metapelite	Fsp, Qz, Bt, Grt, Rt	725 ± 25	0.95 ± 0.05	289.1 ± 6.3	U/Pb (Zrn) ⊖	[153–155]	Avc15
Dent Blanche	Valpelline	Cc metapelite	Grt, Bt, Sil	703 ± 42	0.55 ± 0.1	288 ± 3.9	U/Pb (Zrn) ⊖	[152–154]	Avc24
II DK Zone	Val Sesia	Cc metapelite	Qz, Wm, Grt, Pl, Kfs, Bt, Zrn, Ilm	623 ± 42.5	0.7 ± 0.1	294 ± 4.1	U/Pb (Zrn) ⊖	[154]	Apc26
Silvretta nappe	Ischgl	Un metabasite	Grt, Omp, Qz, Rt, Ms	625 ± 25	2.60 ± 0.3	Carboniferous		[99]	Avco8
Silvretta nappe	Val Puntota	Un metabasite	Grt, Omp, Qz, Rt, Ms	475 ± 25	2.60 ± 0.1	Carboniferous		[99]	Avco9
Silvretta nappe	Hochnoerderer	Un metabasite	Grt, Hbl, Cpx, Pl, Qz	640 ± 40	0.65 ± 0.1	Carboniferous		[156–158]	Avco10
Silvretta nappe	Various	Un metabasite	eclogitic assemblage	655 ± 15	2.80	351 ± 22	Sm/Nd (WR) ⊙	[159]	Avco11
Silvretta nappe	Pischahorn	Cc metapelite	Qz, Ms, And	600	0.20	Carboniferous		[157,160]	Avc11
Languard-Campo	Sondalo	Cc metapelite	Sil, Opx, Kfs, Bt, Qz	660 ± 90	0.5 ± 0.1	290 ± 2	Sm/Nd (WR) ⊙	[161,162]	Apc7
Languard-Campo	Mortirolo	Cc metapelite	Dum, Qz	800 ± 50	2.00	Devonian		[93]	Avc12
Languard-Campo	Mortirolo	Cc metapelite	Di, Grt, Scp, Pl, Qz	850 ± 100	0.77 ± 0.12	Carboniferous		[95]	Avc13
Languard-Campo	Mortirolo	Cc metapelite	Bt, St, Wm, Grt, Pl, Qz, Rt, Ilm, Tur	620 ± 40	0.9 ± 0.2	Dev.-Carb.		[98]	Avc16
Languard-Campo	Mortirolo	Cc metapelite	Bt, Sil, Grt, Pl, Qz, Rt, Ilm	815 ± 35	0.80 ± 0.2	Dev.-Carb.		[98]	Avc17
Languard-Campo	Mortirolo	Cc metapelite	Grt, St, Wm, Bt, Pl, Qz, Ilm	600 ± 20	0.60 ± 0.01	Dev.-Carb.		[163]	Avc18
Oetztal–Stubai	Silandro	Cc metapelite	Grt, Sil, And, Bt, Pl, Qz, Crd	605 ± 35	0.42 ± 0.1	290 ± 17	Rb/Sr (WR) ⊙	[164,165]	Apc9a
Oetztal–Stubai	Lagenfeld	Un metabasite	Grt, Omp	750 ± 50	2.70 ± 0.2	350 ± 8	Sm/Nd (Gr) ⊙	[97,166]	Avo3
Oetztal–Stubai	Burg	Cc metapelite	Grt, Wm, Pl, Qz, St, Ky	600 ± 50	1.20 ± 0.1	355 ± 5	Th/U/Pb (Mnz) ⊕	[167]	Avc4
Oetztal–Stubai	Various	Cc metapelite	Pl, Wm, Bt, Qz, Kfs, Grt, Ky	600 ± 50	0.55 ± 0.15	320 ± 58	Th/U/Pb (Mnz) ⊘	[168]	Avc25
Oetztal–Stubai	Kaunertal	Cc metagranitoid	Qz, Kfs, Pl, Wm, Bt, Grt, Ep, Ilm, Ttn	630	0.75 ± 0.1	335.7 ± 9.6	Sm/Nd (Gr-WR) ⊖	[169]	Avc26
Oetztal–Stubai	Alpeiner Valley	Cc metapelite	Qz, Pl, Wm, Bt, Grt, St, Ilm	680 ± 35	1.20 ± 0.1	327.5 ± 12.5	Th/U/Pb (Mnz) ⊕	[170]	Avc27a
Oetztal–Stubai	Alpeiner Valley	Cc metapelite	Qz, Pl, Wm, Bt, Grt, St, Ilm	600 ± 35	0.40 ± 0.1	310 ± 5	Th/U/Pb (Mnz) ⊕	[170]	Avc27b
Oetztal–Stubai	Soelden-Umhausen	Cc metapelite	Qz, Grt, St, Ky, Pl	600 ± 50	1.20 ± 0.1	365 ± 5	Th/U/Pb (Mnz) ⊕	[167]	Avc28a
Oetztal–Stubai	Soelden-Umhausen	Cc metapelite	Qz, Grt, St, Sil, Pl	700 ± 50	0.50 ± 0.1	323 ± 5	Th/U/Pb (Mnz) ⊕	[167]	Avc28b
Ulten Zone	Samemberg Alm	Cc metapelite	Grt, Bt, Pl, Kfs, Ky, Rt	700 ± 50	1.50 ± 0.5	365	Pb/Pb (Zrn) ⊙	[94,171,172]	Avc5
Ulten Zone	Samemberg Alm	Un metabasite	Grt, Omp, Qz	700 ± 50	1.40 ± 0.2	late Devonian		[94]	Avco6
Ulten Zone	Samemberg Alm	Ma ultramafic	Grt-bearing	790 ± 20	2.50 ± 0.3	330 ± 4	Sm/Nd (Grt-CPx-WR) ⊙	[94,96,101,102]	Avo7
Ulten Zone	Samemberg Alm	Cc metapelite	Ky, Grt, Qz, Pl, Bt, Rt	625 ± 25	1.15 ± 0.05	347 ± 4	Th/U/Pb (Mnz) ⊘	[173,174]	Avc19
Ulten Zone	Samemberg Alm	Cc metapelite	Ky, Grt, Qz, Pl, Bt, Rt	720	0.95 ± 0.05	328 ± 2	Th/U/Pb (Mnz) ⊘	[173,174]	Avc20
Ulten Zone	Hochwart	Cc metabasite	Ol, Opx, Sp, Cpx, Amph	790 ± 20	2.50 ± 0.3	330 ± 6	Sm/Nd (Zrn) ⊖	[175]	Avc29
Schobergruppe	Lienz	Cc metapelite	Grt, Qz, Pl, Ms, Bt, St, Chl, Ky	500		321 ± 14	Th/Pb (Mnz) ⊕	[176]	Avc1
Schobergruppe	Barrenlesee	Un metabasite	Grt, Cpx, Amph, Qz, Wm, Im, Ep, Pl	700 ± 50	1.50 ± 0.2	305 ± 5	Lu/Hf (Grt-WR) ⊙	[177]	Avco12
Woelz Unit	Hochgroessen	Oc metabasite	Grt, Omp, Amp, Rt, Ilm, Ep	700 ± 50	2.00 ± 0.2	397 ± 8	Ar/Ar (Amp) ⊙	[158,178]	Avo2
Rappold Unit	Various	Cc metapelite		540 ± 15	0.66 ± 0.08	Carboniferous		[179,180]	Avc23
Saualpe	Various	Cc metapelite	Qz, Grt, Ky, Wm, Pl, St, Bt	575 ± 75	0.50 ± 0.1	320 ± 16	Th/U/Pb (Mnz) ⊕	[181]	Avc30
Lower Austroalpine	Sopron	Cc metapelite	Bt, And, Sil, Qz, Pl	637 ± 62	0.28 ± 0.1	300 ± 40	Th/U/Pb (Mnz) ⊕	[182]	Apc14

Table 3. Rock type for the Penninic domain including the metamorphic assemblages, P-T conditions, and Variscan ages. Cc = continental crust; Oc = oceanic crust; Ma = mantle; Un = undefined crust. Geochronological data acquisition: ⊙ mineral separation; ⊖ mineral separation and trace elements. See reference coding in Appendix A. Mineral abbreviations are after [141].

Tect. Unit	Location	Group	Assemblage	Temp (°C)	Pres (GPa)	Age (Ma)	Method	Refs	Code
Savona Massif	Savona	Cc metabasite	Grt, Omp, Qz, Ms	700 ± 50	1.70	383 ± 9	U/Pb (Zrn) ⊖	[116,120, 122]	Pvc1
Clarea Complex	Cottian Alps	Cc metapelite	Grt, Ms, Pl, Ky, Rt, Qz	600 ± 50	0.95 ± 0.15	350 ± 10	Ar/Ar (Wm) ⊙	[111,183]	Pvc2
Dora-Maira Massif	Punta Muret	Cc metapelite	Qz, Wm, Grt, St, Bi, Ilm	650 ± 10	0.70 ± 0.1	324 ± 6	U/Pb (Mnz) ⊖	[184]	Pvc8
Gran Paradiso Massif	Valnontey	Cc metapelite	Grt, St, Ilm, Qtz	625 ± 25	0.60 ± 0.1	Dev.-Carb.		[185]	Pvc3
Monte Rosa Massif	Gressoney Valley	Cc metapelite	Grt, Qz	562 ± 12	0.50 ± 0.1	Dev.-Carb.		[186]	Pvc5
Mischabel nappe	Siviez	Cc metabasite	Hbl, Pl, Qz	600 ± 50	0.55 ± 0.05	Dev.-Carb.		[103,109]	Pvc7
Adula nappe	Trescolmen	Un metabasite	Grt, Omp, Ms, Amp, Qz, Chl	750 ± 75	2.20 ± 0.25	374 ± 28	U/Pb (Zrn) ⊖	[119,121]	Pvco8
Adula nappe	Vals, Confin	Un metabasite metagranitoid	Grt, Omp, Ky, Rt, Ms, Ep, Pl, Qz Pl, Qz, Grt, Ms, Ep, Rt	640 ± 75	1.70 ± 0.25	329 ± 25	U/Pb (Zrn) ⊖	[119,121]	Pvco9
Suretta nappe	Avers	Un metabasite	Grt, Hbl, Cpx, Ep, Qz	683 ± 66	2.00	Dev.-Carb.		[118]	Pvco10
Tauren Window	Frosnitztal	Un metabasite	Grt, Omp, Qz	450 ± 50	1.00 ± 0.2	418.5 ± 18.5	Sm/Nd-U/Pb (WR-Zrn) ⊖	[114,117]	Pvco11
Tauren Window	Mallnitz	Un metabasite	Grt, Omp, Qz	620 ± 100	1.20	418.5 ± 18.5	Sm/Nd-U/Pb (WR-Zrn) ⊖	[113,117]	Pvco12

Table 4. Rock type for the Helvetic–Dauphinois–Provençal domain including the metamorphic assemblages, P-T conditions, and Variscan ages. Cc = continental crust; Oc = oceanic crust; Ma = mantle; Un = undefined crust. Geochronological data acquisition: ⊙ mineral separation; ⊖ mineral separation and trace elements. See reference coding in Appendix A. Mineral abbreviations are after [141].

Tect. Unit	Location	Group	Assemblage	Temp (°C)	Pres (GPa)	Age (Ma)	Method	Refs	Code
Argentera Massif	Tinèe	Un metabasite	Grt, Hbl, Cpx, Pl, Qz	735 ± 25	1.30 ± 0.1	Devonian		[134]	Hvco1a
Argentera Massif	Valle Gesso; Valle Stura; Vésubie	Un metabasite	Grt, Hbl, Cpx, Pl, Qz	735 ± 25	1.30 ± 0.1	Devonian		[134]	Hvco1b
Argentera Massif	Passo della Mena, Frisson lakes	Cc metapelite	Grt, Hbl, Cpx, Pl, Qz, Rt/Ilm	735 ± 15	1.38 ± 0.05	340 ± 4	U/Pb (Zrn) ⊖	[137,187]	Hvc2
Argentera Massif	Various	Un metabasite	Grt, Hbl, Cpx, Pl, Qz	735 ± 25	1.30 ± 0.1	Devonian		[134]	Hvco16
Argentera Massif	Various	Un metabasite	Grt, Hbl, Cpx, Pl, Qz	735 ± 25	1.30 ± 0.1	Devonian		[134]	Hvco17
Argentera Massif	Lac Long	Oc metabasite	Cpx, Pl, Amph, Grt, Rt, Ilm	690 ± 55	1.50 ± 0.25	>339.7 ± 12	Ar/Ar (Amp) ⊖	[138]	Hvo17a
Argentera Massif	Lago Valscura	Oc metabasite	Cpx, Pl, Amph, Grt, Rt, Ilm	690 ± 55	1.50 ± 0.25	>339.7 ± 12	Ar/Ar (Amp) ⊖	[138]	Hvo17b
Argentera Massif	Various	Un metabasite	Grt, Hbl, Cpx, Pl, Qz	735 ± 25	1.30 ± 0.1	Devonian		[134]	Hvco18
Argentera Massif	Various	Un metabasite	Grt, Hbl, Cpx, Pl, Qz	735 ± 25	1.30 ± 0.1	Devonian		[134]	Hvco19
Pelvoux Massif	La Lavey	Un metabasite		850 ± 50	1.40 ± 0.1	Devonian		[188,189]	Hvco7
Pelvoux Massif	Peyre Arguet	Un metabasite	Cpx, Grt, Pl, Prg, Rt, Qz	800 ± 50	0.50 ± 0.2	Dev.-Carb.		[188–190]	Hvco8
Pelvoux Massif	La Lavey	Un metabasite	Grt, Cpx, Qz, Rt, Pl, Amph, Bt	690 ± 40	1.60 ± 0.1	337.5 ± 7.5	U/Pb (Rt) ⊖	[191]	Hvco21a

Table 4. *Cont.*

Tect. Unit	Location	Group	Assemblage	Temp (°C)	Pres (GPa)	Age (Ma)	Method	Refs	Code
Pelvoux Massif	La Lavey	Un metabasite	Cpx, Qz, Pl, Amph	835 ± 35	0.75 ± 0.15	315.5 ± 21.5	U/Pb (Zrn) ⊖	[191]	Hvco21b
Pelvoux Massif	Valgaudemar Valley	Ma ultramafic	Grt-bearing	1055 ± 85	3.50 ± 0.5	Devonian		[192]	Hvco23
Grandes Rousses	Romanche Valley	Un metabasite	Cpx, Grt, Qz, Rt	717 ± 67	0.55 ± 0.15	321 ± 10	Ar/Ar (Amp) ⊙	[193]	Hvco5
Grandes Rousses	Oisan	Un metabasite	Cpx, Grt, Qz, Rt	884 ± 109	1.30 ± 0.4	Dev.-Carb.		[193]	Hvco6
Belledonne Massif	Lac de la Croix	Un metabasite	Grt, Cpx, Pl, Qz, Rt Grt, Hbl, Cpx, Qz, Rt, Zo	640 ± 30	1.20 ± 0.1	Devonian		[189]	Hvco9
Belledonne Massif	Allemond	Cc metapelite	Grt, St, Bt, Ms, Chl, Pl, Qz, Rt	550 ± 50	1.00 ± 0.1	Devonian		[23,194]	Hvc3
Belledonne Massif	Livet	Cc metapelite	Gt, St, Bt, Ms, Pl, Qz, Ilm	590 ± 60	0.80 ± 0.2	352 ± 55	K/Ar (Amp) ⊙	[23,194,195]	Hvc4
Belledonne Massif	Grand Mont	Cc metapelite	Qz, Pl, Bt, Grt, Rt	740 ± 40	1.20 ± 0.2	322 ± 12.5	U/Pb (Zrn) ⊖	[126]	Hvc16b
Belledonne Massif	Grand Mont	Cc metapelite	Qz, Pl, Bt, Grt, Ilm	650 ± 50	0.95 ± 0.15	Carboniferous		[126]	Hvc16a
Belledonne Massif	Grand Mont	Cc metapelite	Qz, Pl, Bt, Grt, Ilm	580 ± 30	0.65 ± 0.15	306 ± 3	U/Pb (Zrn) ⊖	[126]	Hvc16c
Belledonne Massif	Taillefer	Cc metapelite	Qz, Wm, Pl, Bt, St, Grt, Ky	608 ± 14	0.58 ± 0.06	337 ± 7	U/Pb (Zrn) ⊙	[196]	Hvc17
Belledonne Massif	Grand Mont	Un metabasite	Grt, Cpx, Qz, Rt, Amp	715 ± 25	1.50 ± 0.1	340 ± 11	U/Pb (Rt) ⊖	[126]	Hvco20a
Belledonne Massif	Grand Mont	Un metabasite	Grt, Cpx, Amp, Ilm, Pl, Qz	580 ± 30	0.65 ± 0.15	306 ± 3	U/Pb (Zrn) ⊖	[126]	Hvco20b
Aiguilles Rouges	Lac Cornu	Un metabasite	Grt, Cpx, Hbl, Qz, Rt	737 ± 12	1.55 ± 0.05	Devonian		[124,133]	Hvco10
Aiguilles Rouges	Col de Bérard	Cc metapelite	Grt, Ms, Ky, Qz, Pl	650 ± 25	1.30 ± 0.1	Carboniferous		[197]	Hvc11
Aiguilles Rouges	Emosson lake	Cc metapelite	Bt, Qz, Kfs, Pl, Ms, Gt	550 ± 25	0.90 ± 0.1	Carboniferous		[198]	Hvc12a
Aiguilles Rouges	Emosson lake	Cc metapelite	Bt, Qz, Kfs, Pl, Ms, Gt	650 ± 20	0.31 ± 0.01	320 ± 1	U/Pb (Mnz) ⊙	[198,199]	Hvc12b
Aiguilles Rouges	St-Gervais-les-Bains	Cc metapelite		700 ± 50	1.00 ± 0.15	Dev.-Carb.		[200]	Hvc15
Aiguilles Rouges	Lac Cornu	Un metabasite	Amp, Grt, Cpx, Qz, Rt	700 ± 50	1.75 ± 0.15	337.5 ± 2.5	U/Pb (Rt) ⊖	[127]	Hvco22a
Aiguilles Rouges	Lac Cornu	Un metabasite	Amp, Grt, Cpx, Pl, Qz, Ilm	650 ± 50	0.95 ± 0.15	Carboniferous		[127]	Hvco22b
Mont Blanc Massif	Martigny	Cc metabasite skarn	Hbl, Grt, Qz, Pl Grt, Mag, Di, Hd	544 ± 45	0.68 ± 0.07	321 ± 14	Ar/Ar (Amp) ⊙	[201]	Hvc13
Aar Massif	Susten Pass	Cc metapelite				330 ± 3	U/Pb (Zrn) ⊙	[123,202]	Hvc14

4. Metamorphic Evolution

The distribution of absolute ages together with evolutionary paths of metamorphism (Figures 4–6) identifies three main tectonic stages for the Variscan history of the Alpine area [63]: Devonian (420–370 Ma—early Variscan), late Devonian–late Carboniferous (370–330 Ma—middle Variscan), and late Carboniferous–early Permian (330–290 Ma—late Variscan).

4.1. Devonian (420–370 Ma)

Scarce Devonian tectonometamorphic relicts are found in all the Alpine domains (Figure 4a). Eclogites from the Penninic and Austroalpine domains (Adula nappe, Savona Massif, and Woelz Unit; [116,119–121,158,178]), characterized by garnet, omphacite, and rutile mineral association, and metapelites with dumortierite in the Languard-Campo nappe (central Austroalpine domain; [93]) document eclogite facies conditions (Figure 4a,b). Similarly, metabasites containing garnet, clinopyroxene, amphibole, and plagioclase are described in the Argentera, Pelvoux, and Aiguilles Rouges Massifs in the Helvetic–Dauphinois–Provençal domain. The symplectites of clinopyroxene and plagioclase replacing omphacite document the re-equilibration of eclogite facies conditions or HP granulite facies con-

ditions [134,203]. The ages of the majority of these metabasites are only geologically constrained (Tables 2–4 and Figure 4a,b). Ep-amphibolite facies conditions are commonly recorded via garnet-chloritoid-biotite-bearing metapelites from the Southalpine domain [71,80,81], garnet-staurolite-biotite-bearing metapelite from the Belledonne Massif [23,194], and metabasite from the Tauren Window [114,117]. In addition, amphibolite facies conditions (Figure 4a,b) are documented via few rocks in the Tauren Window (Penninic domain; [113,117]) and Belledonne Massif (Helvetic–Dauphinois–Provençal domain; [189]).

The Devonian metamorphic imprint developed under a general low to moderate T/P ratio which indicates Franciscan to cold Barrovian metamorphic field gradients (Figure 4c). The coldest thermal states are documented with rocks from the Austroalpine and Penninic domains. Rocks from the Southalpine and Helvetic–Dauphinois–Provençal domains record a cold Barrovian metamorphic field gradient (Figure 4c).

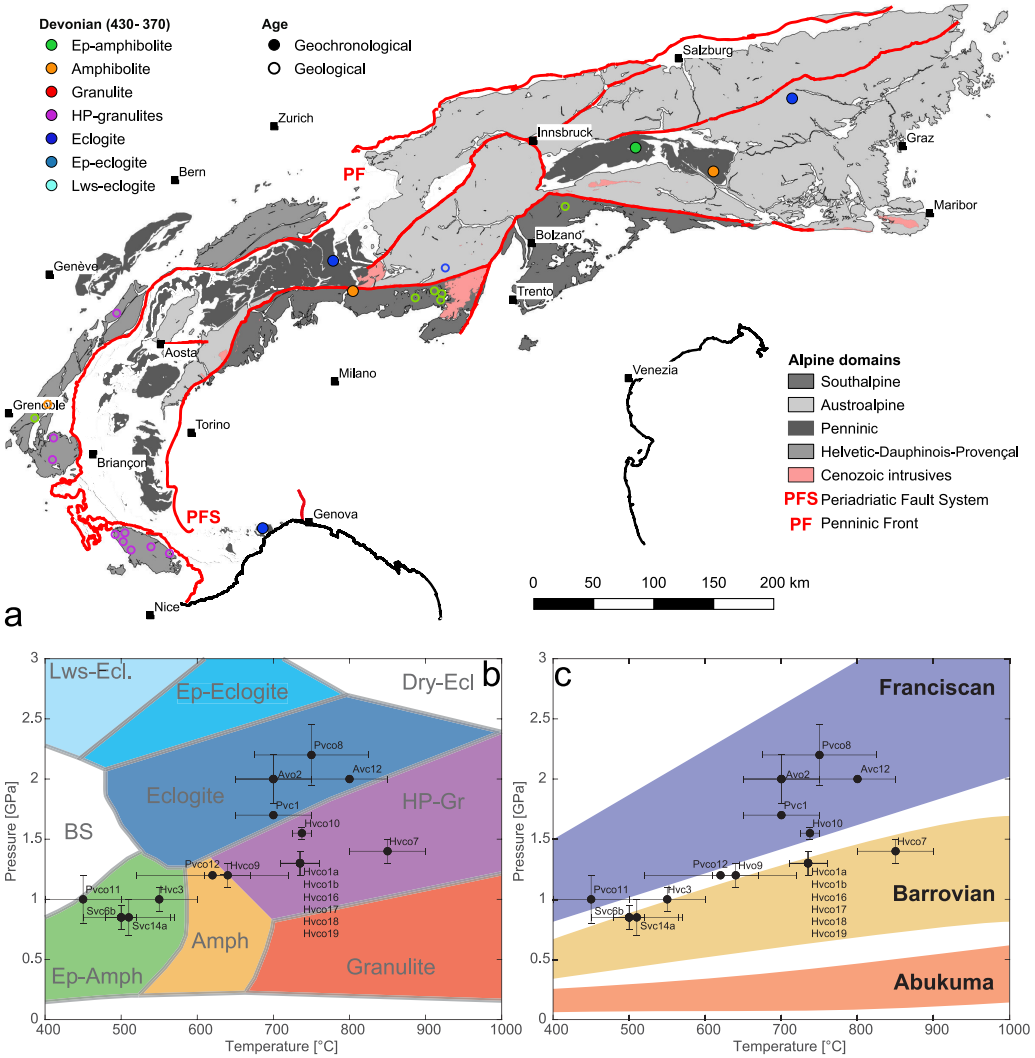

Figure 4. (**a**) Devonian metamorphic imprints and geochronological and geological ages. (**b**) PT data of Devonian samples and relative metamorphic facies (modified after [43,204,205]). (**c**) PT data of Devonian samples and relative metamorphic field gradients (modified after [35,204]). See reference coding in Appendix A and codes information in Tables 1–4.

4.2. Late Devonian–Late Carboniferous (370–330 Ma)

Abundant relicts with a late Devonian to late Carboniferous metamorphic imprint occur in the central and western Alps (Figure 5a). In the Helvetic–Dauphinois–Provençal domain, the metamorphic imprint generally developed under HP granulite facies conditions (Figure 5a,b) with the mineral association characterized by garnet, clinopyrox-

ene, and amphibole in metabasites and quartz, garnet, and kyanite in metapelites (e.g., [77,126,137,138,189]). One sample in the Aiguilles Rouges Massif (Figure 5a,b) still preserves eclogite facies imprints (Lac Cornu—Hvco22a, [127]). Two samples of metapelites in the Belledonne Massif document amphibolite facies conditions (Hvc4 and Hvc17; Figure 5a,b) characterized by quartz, garnet, and staurolite mineral association [194–196]. Ep-amphibolite and granulite facies conditions are documented in two cases from the Aiguilles Rouges and Pelvoux Massifs, respectively [188,198], but no radiometric age is available (Figure 5a,b).

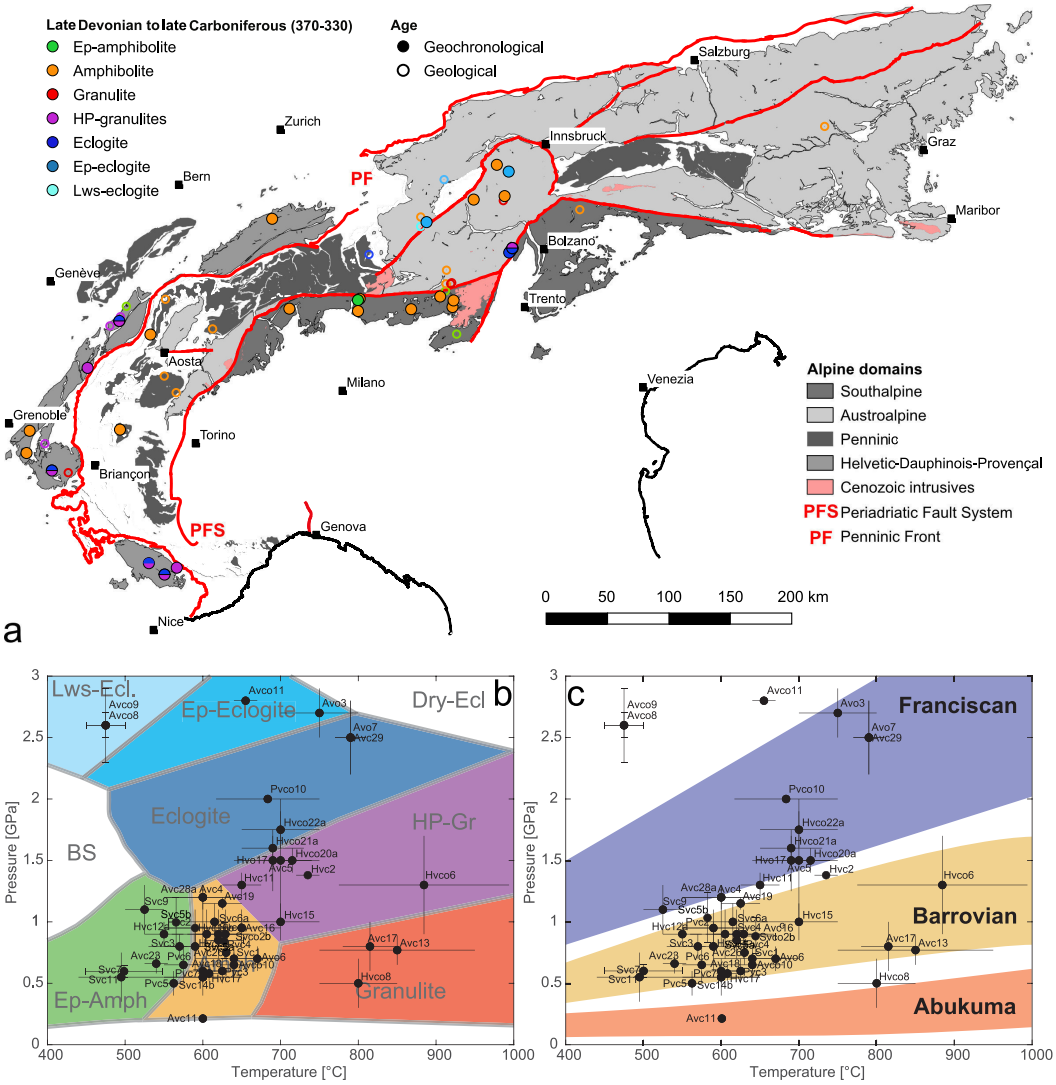

Figure 5. (**a**) Late Devonian–late Carboniferous metamorphic imprint and age types (geochronological and geological age). (**b**) PT data of Late Devonian–late Carboniferous samples and relative metamorphic facies (modified after [43,204,205]). (**c**) PT data of Late Devonian–late Carboniferous samples and relative metamorphic field gradients (modified after [35,204]). See reference coding in Appendix A and codes information in Tables 1–4.

Rocks from the Penninic domain commonly indicate amphibolite facies conditions for the late Devonian to late Carboniferous metamorphic imprints (Figure 5a,b) with metapelites characterized by quartz, garnet, and staurolite assemblages [110,183,185,186,206] and metabasites by garnet, amphibole, and clinopyroxene mineral associations [103,109,118]. In the Austroalpine domain, the late Devonian to late Carboniferous metamorphic imprint lies in different conditions. Eclogite, Ep-eclogite, and Lws-eclogite facies conditions are documented with metabasites from the Oetztal–Stubai Complex and Silvretta nappe (Figure 5a,b), all supported by radiometric age [92,94,99,101,102,159,166,175]. Amphi-

bolite facies conditions are instead documented with metapelites and metabasites from the same units and from the Languard-Campo nappe [94,98,156,158,163,167,169,173,179]. In the latter unit, granulite facies conditions are recorded with metapelites in the Mortirolo area, but their age is estimated only by geological constraints [95,98]. In the Southalpine domain, amphibolite and Ep-amphibolite facies conditions are documented with metapelites across the Orobic basement and Strona-Ceneri unit, characterized by quartz, garnet, biotite, staurolite, and minor kyanite mineral associations [71,78,80–82,84,142,144,146,148].

The late Devonian–late Carboniferous metamorphic imprint developed under a general moderate T/P ratio, especially in the Penninic and Southalpine domains, resulting in a Barrovian metamorphic field gradient (Figure 5c). However, some rocks in the central Austroalpine and Helvetic–Dauphinois–Provençal domains document a colder thermal state that points to the Franciscan metamorphic field gradient (Figure 5c).

4.3. Late Carboniferous–Early Permian (330–290 Ma)

Most of the rocks that recorded late Carboniferous to early Permian metamorphism are derived from the continental crust (metapelites and paragneisses). The metamorphic imprint during this period was dominated by (HP) granulites and amphibolites facies conditions (Figure 6a,b), with only a few exceptions such as the record of Ep-amphibolite facies in the Belledonne Massif from the Helvetic–Dauphinois–Provençal domain [126]. A unique case is represented by the metabasite from Vals in the Adula nappe (Penninic domain) that documents eclogite facies conditions (Figure 6a,b, [119,121]). However, the radiometric estimate of 329 ± 25 Ma suggests a possible early Carboniferous age for the metamorphism recorded with this rock.

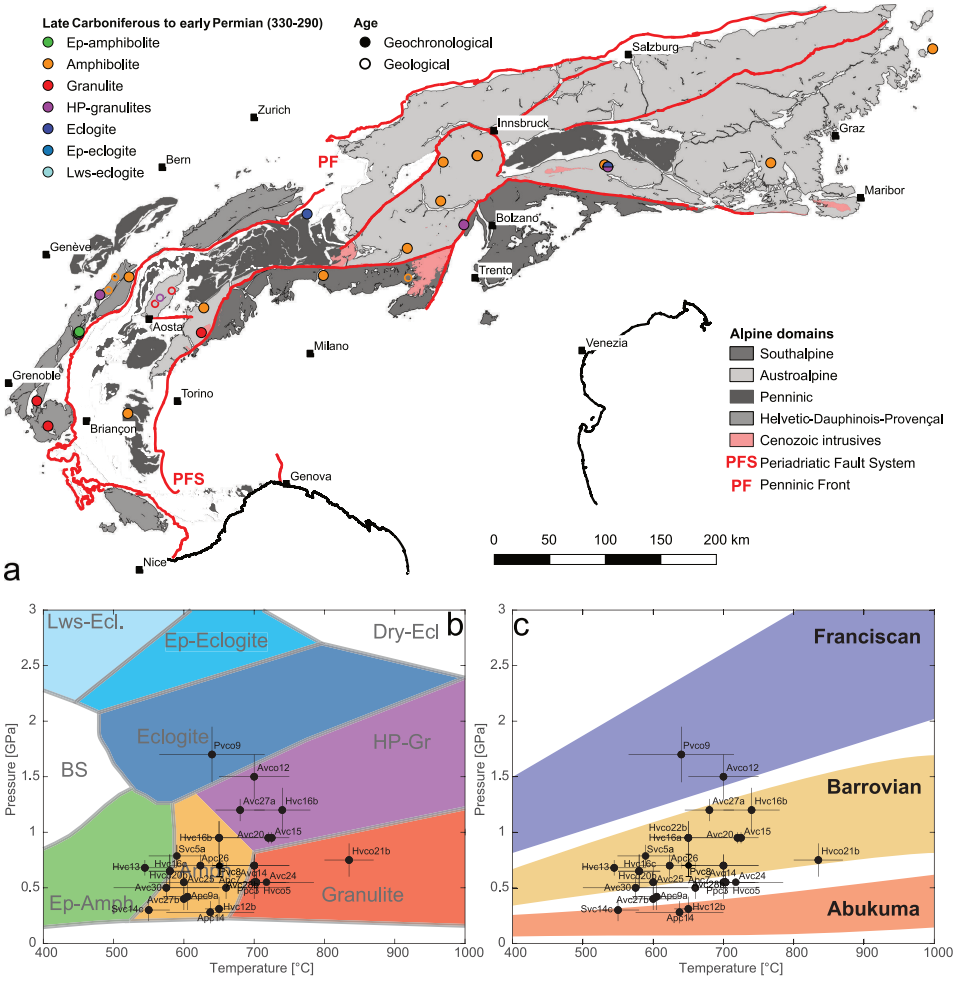

Figure 6. (**a**) Late Carboniferous–early Permian metamorphic imprint and age types (geochronological and geological age). (**b**) PT data of Late Carboniferous–early Permian samples and relative

metamorphic facies (modified after [43,204,205]). (**c**) PT data of Late Carboniferous–early Permian samples and relative metamorphic field gradients (modified after [35,204]). See reference coding in Appendix A and codes information in Tables 1–4.

Therefore, the late Carboniferous to early Permian metamorphic imprint developed under a moderate to high T/P ratio that indicates a Barrovian to Abukuma metamorphic field gradient (Figure 6c). Two exceptions are represented by rocks from the Adula nappe in the Penninic domain and Schobergruppe in the Austroalpine domain that point to a Franciscan metamorphic field gradient (Figure 6c).

4.4. Metamorphic Field Gradients

The Franciscan field gradient is the typical gradient that characterizes the subduction zones (e.g., [36,205,207]). The PT conditions of Variscan rocks documenting a Franciscan field gradient indicate a thermal gradient lower than 20 °C/km (blue area in Figure 7) and plot over the PT estimates from worldwide exhumed blueschists and eclogites of subduction complexes (Figure 8). This field gradient characterizes the Devonian evolution of Variscan rocks in the majority of the Alpine domains. The Barrovian field gradient (yellow in Figure 7), which is traditionally interpreted as the effect of crustal thickening during continental collision (e.g., [41,205,208–212]), is recorded in all domains of the Alps since the late Devonian period. The Abukuma field gradient (red in Figure 7) testifies to an abnormally high thermal regime typical of arc systems, ridge settings [42,205,213,214], or thinned lithosphere [205,215] and preferentially developed during the late Carboniferous–early Permian period.

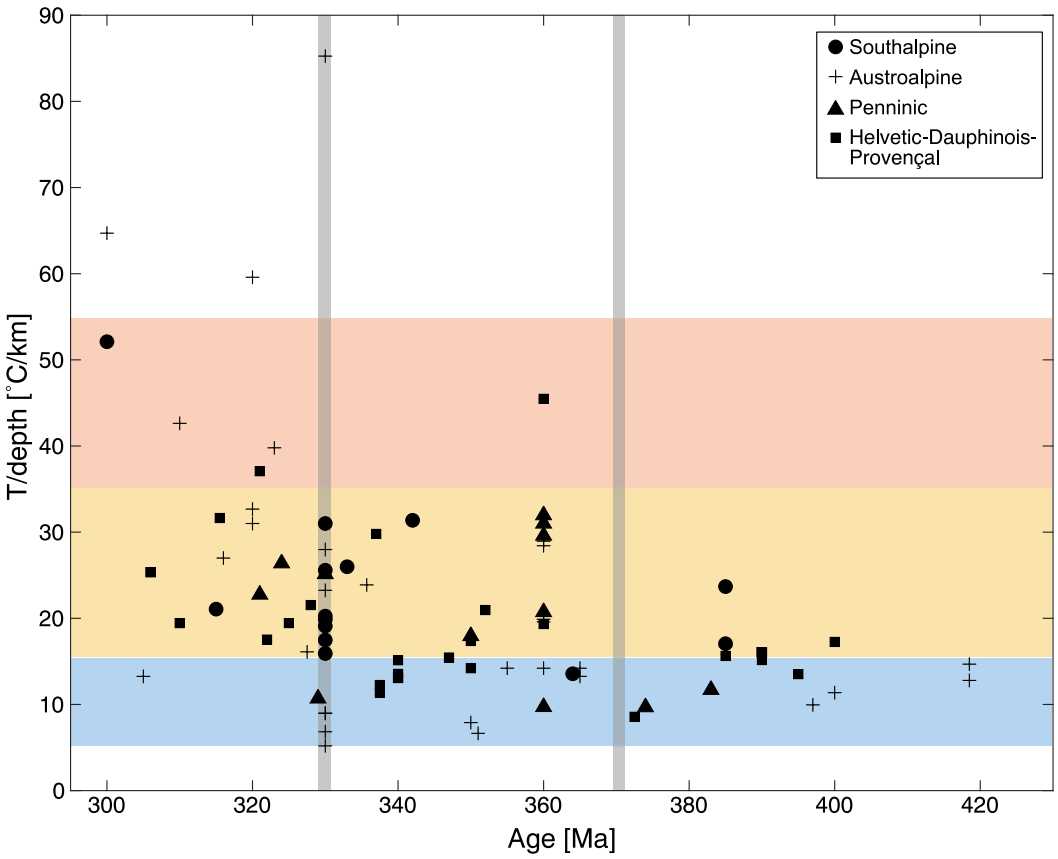

Figure 7. Age vs. geothermal gradient of Variscan rocks in the different domains of the Alps extrapolated from PT conditions, using a reference density of 2900 kg/m^3 (see Table 1). Blue, yellow, and red areas refer to Franciscan, Barrovian, and Abukuma field gradients, respectively.

In particular, during the Devonian time, rocks from the eastern Austroalpine and Penninic domains developed under Franciscan-type conditions (Figure 9a), whereas rocks from the Helvetic–Dauphinois–Provençal and Southalpine domains fell along the upper Barrovian field gradient (Figure 9b). However, in the case of the Helvetic–Dauphinois–Provençal domain, the radiometric estimates are rather old and obtained with obsolete methods [203], and they may represent a mixing of different ages [139], whereas in the Southalpine domain, the ages are mainly constrained on geological criteria.

During the late Devonian–late Carboniferous time, the majority of central Austroalpine and Helvetic–Dauphinois–Provençal rocks still recorded Franciscan-type imprints that are also testified to via one rock from the Southalpine and one from the Penninic domain (Figure 9a). On the contrary, the majority of Southalpine and Penninic rocks re-equilibrated under Barrovian-type conditions that also affected a few rocks from the Austroalpine and Helvetic–Dauphinois–Provençal domains (Figure 9b).

Finally, for the late Carboniferous–early Permian time, only one rock from the eastern Austroalpine domain documents a Franciscan-type imprint, whereas a Barrovian field gradient is recorded via rocks from the Helvetic–Dauphinois–Provençal domain. Rocks from the eastern and western Austroalpine domain document metamorphic field gradients at the transition between low Barrovian and Abukuma, together with a few rocks from the Southalpine and Helvetic–Dauphinois–Provençal domains (Figure 9c).

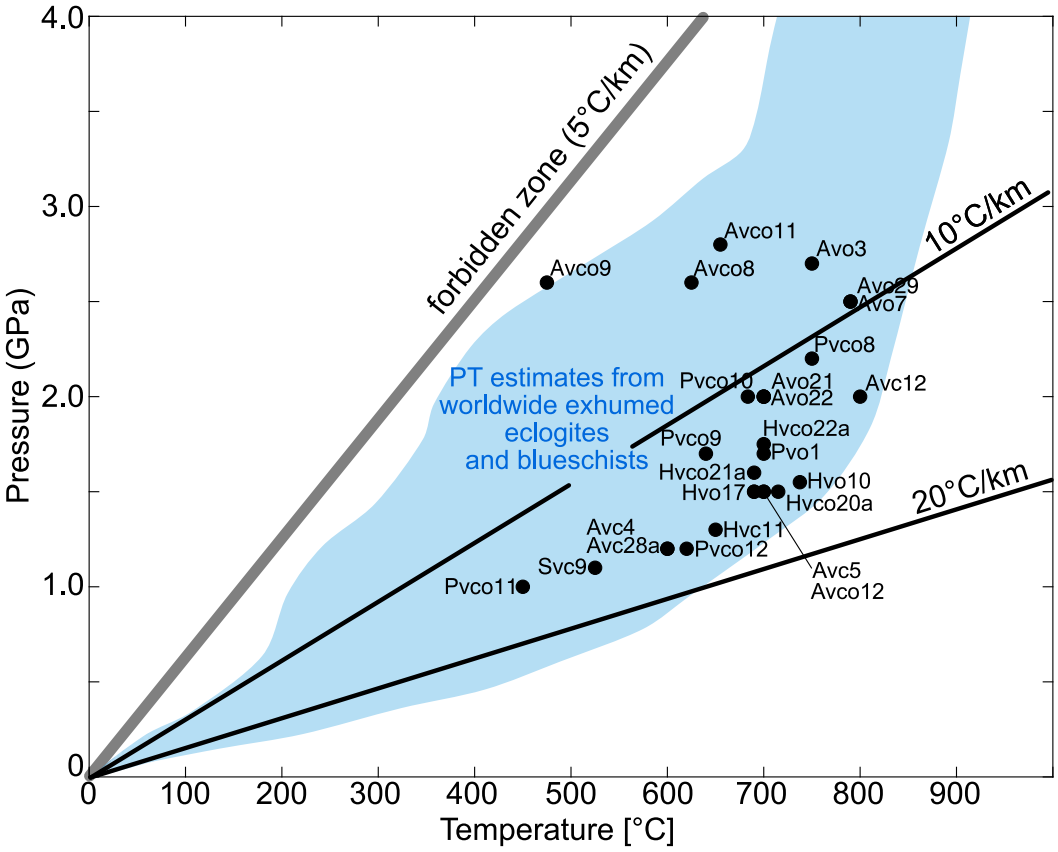

Figure 8. PT estimates of Variscan rocks characterized by Franciscan field gradients. The blue area is the interpolation of PT estimates from worldwide exhumed blueschists and eclogites after [216].

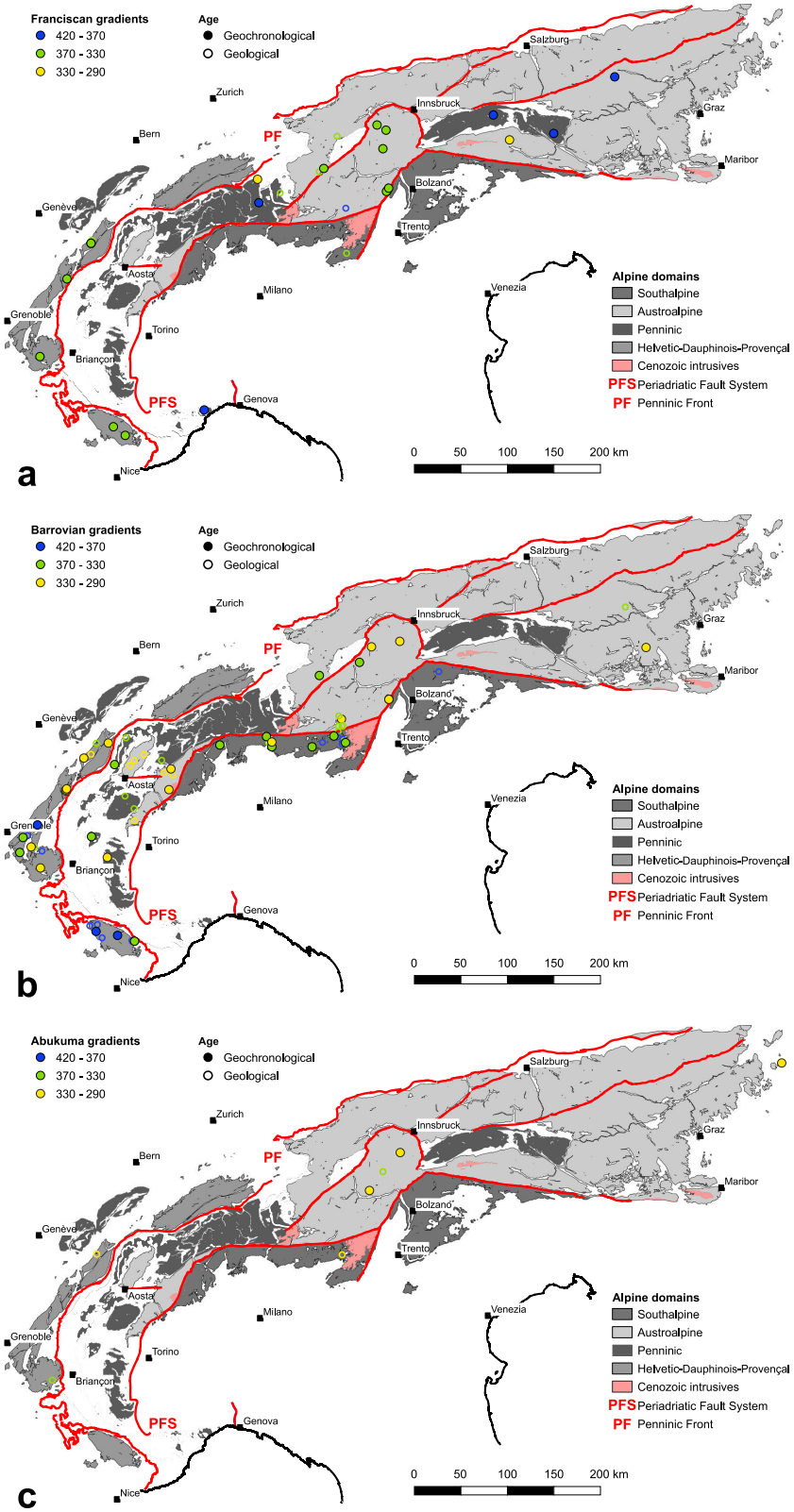

Figure 9. Franciscan (**a**), Barrovian (**b**), and Abukuma (**c**) field gradients calculated for the collected samples as a function of age (blue: Devonian; green: late Devonian–late Carboniferous; yellow: late Carboniferous–early Permian) and location along the Alpine chain.

5. Discussion

The compilation of PT data from Variscan rocks from the Alps highlights the high variability of geothermal gradients as a function of timing and location across the chain

even within a single tectonic domain (Figure 9). This variability is clearly the result of transposition, deformation, translation, and metamorphic overprinting caused by successive tectonic events that characterized the Alpine area from the Permian period to the present day. In particular, Variscan rocks were restructured during the Permian–Mesozoic continental rifting and oceanization and subsequent Alpine subduction and collision. In contrast, other parts of the European Variscan orogen are either not affected or only partially affected by successive tectonometamorphic events, allowing for the preservation of tectonic domains that can be correlated though the different portions of the Variscan belt across Europe. Taking into account the tectonometamorphic fragmentation consequent to successive tectonic events, we tentatively compare the metamorphic imprints and field gradients of Variscan rocks in the different Alpine domains with those in the European domains across three main tectonic stages individuated in Variscan history: Devonian, late Devonian–late Carboniferous, and late Carboniferous–early Permian (Table 5).

During the Devonian period, eclogite and HP granulite facies conditions, developed under Franciscan and upper-Barrovian gradients, dominated the rocks in the Helvetic–Dauphinois–Provençal, Penninic, and Austroalpine domains. Similar metamorphic conditions are described in rocks from the allochthon of the European Variscan massifs, except for the Vosges–Black Forest. In the Southalpine domain, Ep-amphibolite and amphibolite facies conditions dominated during the Devonian period, indicating a general Barrovian metamorphic gradient, which is not described in the European Variscan domains for this period. However, most of the age data in the Southalpine domain are based on geological criteria, with the only geochronological data obtained more than four decades ago [76].

During the late Devonian–late Carboniferous period, HP granulite and eclogite facies conditions still dominated the rocks in the Helvetic–Dauphinois–Provençal and Austroalpine domains, and similar conditions are recorded in rocks from the allochthon of the Vosges–Black Forest and Maures–Estérel–Corsica–Sardinia massifs. For the same period, amphibolite facies conditions, developed under a Barrovian metamorphic field gradient, are recorded in rocks from the Penninic and Southalpine domains and, in the latter, an eclogite facies imprint is not described. The metamorphic outline of the Southalpine domain is similar to that recorded via rocks from the relative autochthon of the Bohemian and Vosges–Black Forest massifs and in the para-autochthon of the Maures–Estérel–Corsica–Sardinia and of the French Central massifs. It must be underlined that exclusively in the relative autochthon of the Bohemian Massif eclogite facies imprint was recorded for the Variscan evolution.

During the late Carboniferous–early Permian period, Variscan rocks in the Helvetic–Dauphinois–Provençal, Austroalpine, and Southalpine domains were characterized by the occurrence of granulite facies conditions and Barrovian to Abukuma metamorphic field gradients. Similar conditions were recorded in rocks from the allochthon of the Vosges–Black Forest and Maures–Estérel–Corsica–Sardinia Massifs, as well as in all domains of the French Central Massif. Amphibolite facies conditions and Barrovian metamorphic field gradients dominate the Variscan rocks from the Penninic domain as well as the allochthon of the Bohemian Massif.

As previously mentioned, the comparison between Variscan rocks in the Alps and European massifs is challenging due to the very different tectonic evolutions that characterized these areas from the Permian period to the present day. Based on metamorphic imprints and field gradients recorded in Variscan rocks, we note that the Helvetic–Dauphinois–Provençal, Austroalpine, and part of the Penninic domains show an evolution roughly similar to that of the mid-Variscan allochthon units, while the evolution of the Southalpine domain is more similar to that of the autochthon units of the European massifs, excluding the eclogite-bearing Bohemian Massif. The Penninic domain lacks late Carboniferous–early Permian granulite facies conditions, consistent with the relative autochthon units of the Vosges–Black Forest Massif and para-autochthon of the Maures–Estérel–Corsica–Sardinia Massif, as well as all domains of the Bohemian Massif.

An interesting output of this review includes the comparison between the Variscan tectonic evolution suggested via metamorphic imprints and field gradients of rocks from the Alps with the scenarios proposed for the evolution of the Variscan orogen in Europe. A Franciscan field gradient (Figure 7; 5–15 °C/km), suggesting the evolution of rocks within a subduction zone, developed during the Devonian period preferentially in the eastern Alps. In the central-western Alps, this gradient mainly developed during the late Devonian to late Carboniferous period (Figure 9a). The oldest age determinations (>380 Ma) are at present considered outdated, given recent estimates in the Helvetic–Dauphinois–Provençal domain [126,138,191,196] and in the other European Variscan massifs (e.g., [139,217–219]).

Table 5. Dominant metamorphic facies and field gradients for the Variscan rocks in Alpine and main European Variscan domains. The > symbol indicates a decrease in the relative abundance of rocks recording the indicated metamorphic conditions.

		ALPINE TECTONIC DOMAINS				VARISCAN TECTONIC DOMAINS							
		ALPS				BOHEMIAN MASSIF		VOSGES–BLACK FOREST		FRENCH CENTRAL MASSIF		MAURES–ESTÉREL–CORSICA–SARDINIA	
		HDP	P	A	S	Mid-Variscan Allochton	Relative Autochton	Mid-Variscan Allochton	Relative Autochton	Mid-Variscan Allochton	Para-Autochton/ Autochton	Mid-Variscan Allochton	Para-Autochton/ Autochton
Devonian (420–365)	Facies	HPG>EA-A	E>EA-A	E	EA>A	E>G>A	E>A>EA>Gs			E>HPG>A		E?	
	Field gradient	uB>F	F>uB	F	uB-B	F-uB	F-B			F-uB		F?	
Late Devonian–late Carboniferous (365–330)	Facies	HPG-E>A>EA	A>E	E>A>G>HPG	A>EA>Gs-LG-UnM	HPG>A>EA	A>EA>Gs	A>HPG>E>EA>Gs	A>EA>Gs	A>HPG>G>Gs	Gs	A>HPG>E>EA	A>EA>Gs
	Field gradient	F>uB>B>A	B>uB>F	F>uB-B>A	uB-B>F	B-uB	B	F-uB-B	B	B>uB	B	F-uB-B	B
Late Carboniferous–Early Permian (330–290)	Facies	A>G>EA>HPG	A>E	A>G>HPG>E	A-Gs>G	A>EA	Gs	A>EA>G	Gs	A>EA>G>Gs	Gs>EA>G>E	A>EA>G	Gs
	Field gradient	B>A	B>F	B-uB>A>F	B-A	B	B	A-B	B	B>A	B>A>uB	A-B	B
References	See references in Tables 1–4 of this work					[9,220–227] [18,19,63,244,261–266]	[220,224,228–231] [18,19,63,244,267]	[232–238] [18–20,241,243,244,268]	[9,11,16,220,239–244] [18–20,35,217,218,269–271]	[9,11,16,217,240,244] [9,11,16,217,240,244]	[9,11,245–248] [16,18–20,219,244,272]	[249–255] [19,273–278]	[253,256–260] [19,274,279–282]

Symbols legend. Alpine tectonic domains: HDP = Helvetic–Dauphinois–Provençal; P = Penninic; A = Austroalpine; S = Southalpine. Metamorphic facies: EA = Ep-amphibolite; A = amphibolite; G = granulite; HPG = HP granulite; E = Eclogite + Ep eclogite + Lws eclogite; GS = greenschist; LG = low grade; UnM = nonmetamorphic. Metamorphic field gradients: F = Franciscan; B = Barrovian; uB = upper Barrovian; A = Abukuma-Buchan.

The preservation of a Variscan subduction zone in the Alpine area is also supported by the age (333–364 Ma; [283,284]) and magmatic arc signature [285] of the gabbroic body of the Ivozio Complex in the Austroalpine domain of the western Alps and by the coeval spinel–garnet transition in Ulten lherzolites. Moreover, the contamination of the subcontinental mantle caused by the Variscan subduction is still identifiable in the distinctive geochemical signature of the Triassic magmatism in the Southalpine domain [286,287]. The coexistence of HP granulite and amphibolite facies assemblages with the eclogite facies assemblage of Franciscan type does not contradict the occurrence of a Carboniferous subduction.

In fact, recent thermomechanical simulations indicate that contrasting metamorphic conditions can simultaneously be observed in different regions of the subduction system [20,205]. The Barrovian field gradient (15–35 °C/km), which is typical for rocks evolving within collisional contexts, developed from Carboniferous to Permian times after the Franciscan gradients or as the re-equilibration of older lower-T relicts (Figure 9b) and is recorded via rocks from all parts of the Alps (Figure 9b). Therefore, all the data indicate a diachronous subduction-related metamorphism, followed by continental collision re-equilibration.

Considering the geodynamic evolution of the Variscan orogeny, there is a general agreement on the closure of an oceanic domain, so called Rheic, and located north of the peri-Gondwanian microblocks (or continental ribbons) during Devonian times [19,288,289]. However, two scenarios are still debated: (i) a single oceanic closure or (ii) several and successive oceanic closures (e.g., the closures of the Rheic, the Saxothuringian, and the Rhenohercynian oceans) [16–18,35,63,224,290].

The Devonian to Carboniferous Franciscan-type assemblages recorded in the Variscan rocks of the Alps may agree with a single oceanic closure characterized by an oceanic subduction with a diachronous burial and exhumation starting from the east, where the oldest Franciscan records occur, and moving westward, where Franciscan records are Carboniferous in age (Figure 9a). This agrees also with the older age of the Barrovian field gradient (i.e., collision) in the central Alps (mainly early Carboniferous) with respect to the western Alps (mainly late Carboniferous; Figure 9b). The monocyclic scenario as proposed for the Bohemian and French massifs accounts for the occurrence of an arc and back-arc system located at present to the north of the Alpine front [271] that would not agree with the records of subduction-type metamorphism in the Variscan rocks of the Alps. Therefore, a more complex subduction geometry has to be considered and tested.

On the other hand, the distribution in age of the Franciscan-type imprints may agree even with a scenario involving several oceanic closures, in which the subduction of an older ocean is testified to in the Penninic and eastern Austroalpine domains of the Alps and the successive subduction of the Saxothuringian ocean is testified to in the central Austroalpine and Helvetic–Dauphinois–Provençal domains (Figure 9a). However, a comparison between P-T-t data and numerical models of mono- and polycyclic scenarios indicates that the latter is the preferred scenario for describing the Variscan orogeny in the Alps [35]. The polycyclic scenario implies that during the Variscan time, the Austroalpine domain was separated into different portions that occupied different palaeogeographic positions. In particular, the eastern Austroalpine domain would have derived from Gondwana or southern Armorica, while the central Austroalpine domain would have belonged to northern Armorica or possibly to Saxothuringian terrains. In the Pelvoux Massif, the Carboniferous age (337 Ma) of HP granulites and the relatively warm thermal gradient estimated for their thermal peak conditions (12–13 °C/km) are interpreted as the thickening of a relatively hot continental crust, presumably caused by the inversion of a Devonian back-arc during the collision [191], rather than a subduction context. However, the obtained PT conditions cannot rule out the possible role of subduction, as PT estimates from worldwide exhumed blueschists and eclogites indicating geothermal gradients from 6 to 20 °C/km for subduction zones (Figure 8). Furthermore, the young U/Pb ages of high-pressure rocks may be subject to uncertainties due to the resetting of the U–Pb system of eclogite facies zircon grains, particularly when they are enclosed within high-temperature country rocks [219].

A similar geothermal gradient has been inferred for Variscan eclogites in the southern Argentera–Mercantour Massif that derives from MORB-type protoliths [138]. This eclogite re-equilibrated under amphibolite facies conditions resulting from the oceanic subduction-related metamorphism developed in this portion of the Helvetic–Dauphinois–Provençal domain [138].

In Figure 10, the geothermal gradients obtained from the PT conditions of Variscan remnants in the Alps, extended up to Triassic times, are reported. From 420 to 370 Ma, the distribution of thermal gradients with age is rather constant around the average value of 15 °C/km. The geothermal gradients almost linearly increase from 370 Ma to reaching the maximum value at ca. 250 Ma and then remain almost constant over the whole Triassic period. This distribution clearly agrees with a sequence of events that starts with subduction (420–370 Ma), continues with continental collision (370–290 Ma), and ends with the continental thinning that resulted in Pangea rifting and the successive drifting of the Alpine Tethys ocean at ca. 160 Ma [61,62,291].

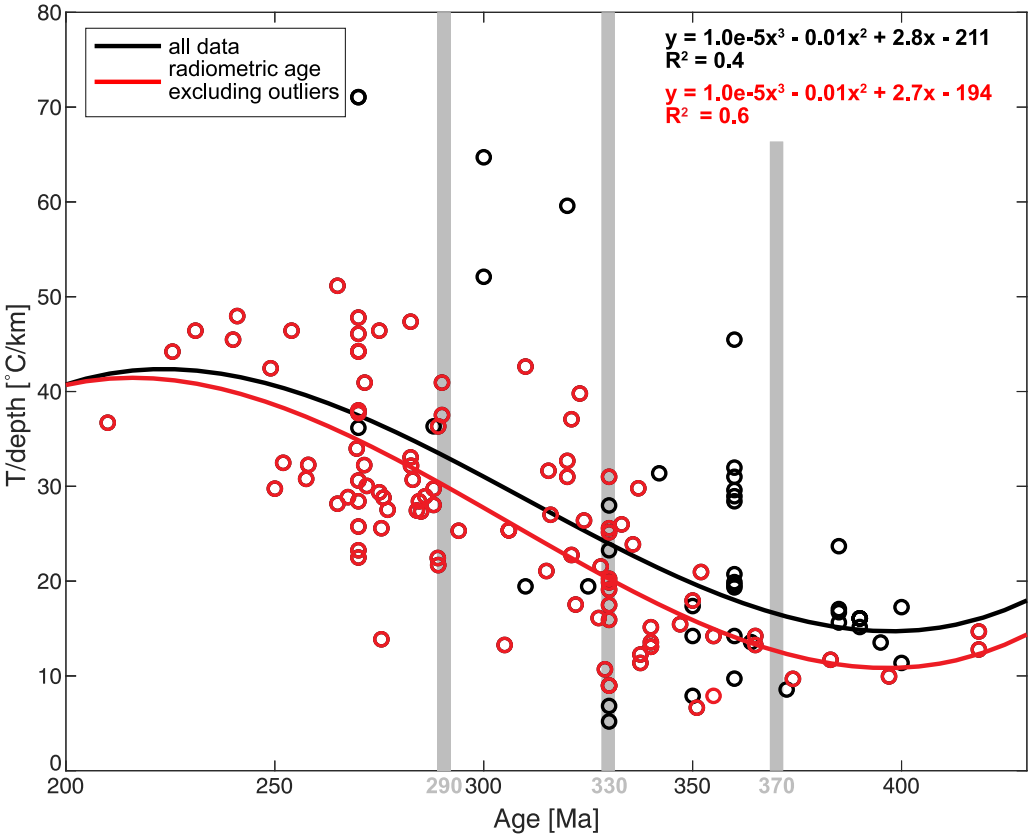

Figure 10. Geothermal gradients obtained from Devonian to Triassic PT conditions of Variscan rocks in the Alps, using a reference density of 2900 kg/m^3. Blue and red lines represent the best interpolation curve for all data and radiometric data only excluding outliers, respectively.

During convergent tectonics, after continental collision and thickening, a phase of gravitational collapse is usually predicted with a thermal balance between deformation-induced and radioactive heat production and heat advection related to continental subduction, orogenic deformation, and magma transfer [215] that results in a decrease, or a reduction of the increase, in geothermal gradients [292]. Interestingly, between 370 and 250 Ma, a significant change in the slope of the interpolation curve is not observed (Figure 10), suggesting the absence of a clear phase of gravitational collapse from the geothermal gradients. This observation leads to different interpretations of the Variscan and post-Variscan evolution in the Alps. One possibility is that it was characterized by a gradual switch from convergence to extension as a result of continental redistribution triggered by the opening of the southern Atlantic ocean [293]. Alternatively, the thermal signature of the

gravitational collapse is not recorded in the Alpine rocks, or it is indistinguishable from the thermal signature of the collision.

6. Conclusions

The compilation of quantitative PT conditions and ages of Variscan rocks from the Alps documents a variable metamorphic evolution across the Alpine domains, spanning from the Devonian to early Permian times. Eclogite and HP granulite facies conditions characterized by geothermal gradients typical of subduction zones occurred in the Penninic and eastern Austroalpine domains during the Devonian period and in the Helvetic–Dauphinois–Provençal and central Austroalpine domains during late Devonian–late Carboniferous time. From the Carboniferous to Permian periods, Barrovian metamorphic field gradients, typical of continental collision, were established in all the Alpine domains.

This metamorphic distribution suggests a pre-Alpine burial of oceanic and continental crust at convergent plate margins, during one or successive oceanic closures. In the single subduction scenario, a diachronic oceanic subduction started from the east and moved westward. In the other scenario, the Devonian subduction of the older ocean was recorded via rocks in the Penninic and eastern Austroalpine domains of the Alps, and the successive Carboniferous subduction of the Saxothuringian ocean was recorded via rocks in the central Austroalpine and Helvetic–Dauphinois–Provençal domains. In either case, the distribution of geothermal gradients from Devonian to Triassic times agree with a sequence of events that starts with subduction, continues with continental collision, and ends with the continental extension that resulted in the Pangea breakup. Whatever the preferred scenario, this review shows that subduction-related metamorphic relicts indicate the occurrence of a Variscan suture in the Alpine domain, and this cannot be neglected in the definition of the tectonic evolution of the European Variscides.

Author Contributions: Conceptualization, M.R. and M.I.S.; methodology, M.R. and M.I.S.; validation, M.R., M.I.S., M.F., J.-M.L., G.R., A.R., D.Z., M.Z. and G.G.; formal analysis, M.R. and M.I.S.; investigation, M.R., M.I.S., M.F., J.-M.L., G.R., A.R., D.Z., M.Z. and G.G.; resources, M.R., M.I.S., M.F., J.-M.L., G.R., A.R., D.Z., M.Z. and G.G.; data curation, M.R., M.I.S. and A.R.; writing—original draft preparation, M.R. and M.I.S.; visualization, M.R.; supervision, M.R., M.I.S., M.F., J.-M.L., G.R., A.R., D.Z., M.Z. and G.G.; funding acquisition, M.R., M.I.S., D.Z. and M.Z. All authors have read and agreed to the published version of the manuscript.

Funding: This research was funded by Piano di sostegno alla ricerca: linea 2, azione A, anno 2021, grant number MRODA-PSR2021.

Data Availability Statement: All data used for this article are present in the tables, figures, and Appendix A of the manuscript.

Acknowledgments: The editor and two anonymous reviewers are gratefully acknowledged for their highly constructive criticism of the text.

Conflicts of Interest: The authors declare no conflict of interest.

Appendix A

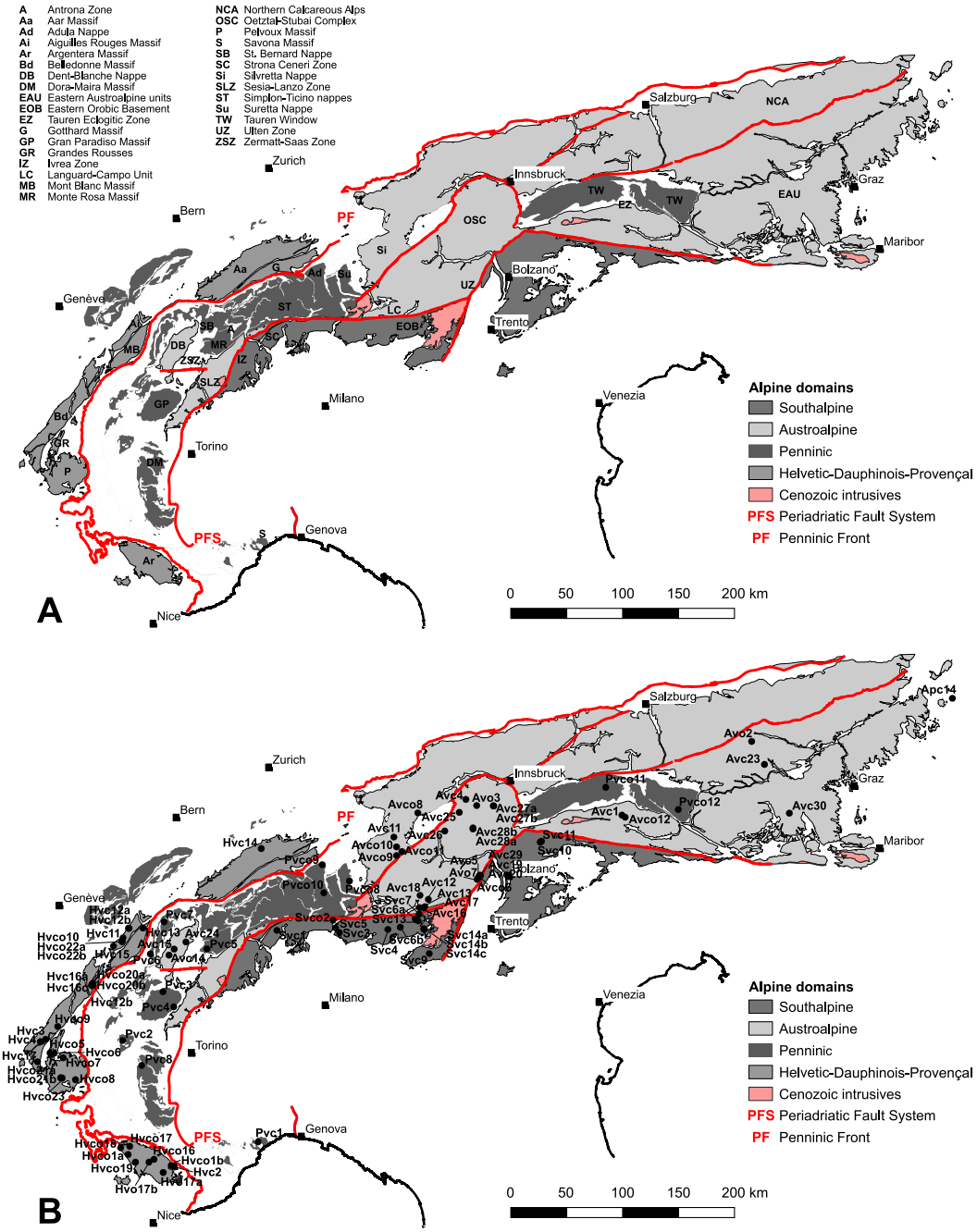

Figure A1. (**A**) Alpine domains, tectonic units and zone, and (**B**) reference coding of collected samples of Tables 1–4.

References

1. Matte, P. Tectonics and plate tectonics model for the Variscan belt of Europe. *Tectonophysics* **1986**, *126*, 329–374. [CrossRef]
2. Ledru, P.; Lardeaux, J.M.; Santallier, D.; Autran, A.; Quenardel, J.M.; Floc'h, J.P.; Lerouge, G.; Maillet, N.; Marchand, J.; Ploquin, A. Ou sont les nappes dans le massif central francais? *Bull. Soc. Geol. Fr.* **1989**, *V*, 605–618. [CrossRef]
3. Oliver, G.J.H.; Corfu, F.; Krogh, T.E. U-Pb ages from SW Poland: Evidence for a Caledonian suture zone between Baltica and Gondwana. *J. Geol. Soc.* **1993**, *150*, 355–369. [CrossRef]
4. Finger, F.; von Quadt, A. U-Pb ages of zircons from a plagiogranite-gneiss in the southeastern Bohemian massif, Austria: Further evidence for an important early Paleozoic rifting episode in the eastern Variscides. *Schweiz. Mineral. Und Petrogr. Mitteilungen* **1995**, *75*, 265–270.

5. Faure, M.; Leloix, C.; Roig, J.Y. Polycyclic evolution of the Hercynian belt; [L'évolution polycyclique de la chaîne hercynienne]. *Bull. Soc. Geol. Fr.* **1997**, *168*, 695–705.
6. Michard, A.; Goffé, B.; Bouybaouene, M.; Saddiqi, O. Late Hercynian–Mesozoic thinning in the Alboran domain: Metamorphic data from the northern Rif, Morocco. *Terra Nova* **1997**, *9*, 171–174. [CrossRef]
7. Tait, J.A.; Bachtadse, V.; Franke, W.; Soffel, H.C. Geodynamic evolution of the European Variscan fold belt: Palaeomagnetic and geological constraints. *Geol. Rundsch.* **1997**, *86*, 585. [CrossRef]
8. Torsvik, T.H. Palaeozoic palaeogeography: A North Atlantic viewpoint. *GFF* **1998**, *120*, 109–118. [CrossRef]
9. Matte, P. The Variscan collage and orogeny (480–290 Ma) and the tectonic definition of the Armorica microplate: A review. *Terra Nova* **2001**, *13*, 122–128. [CrossRef]
10. von Raumer, J.; Stampfli, G.; Borel, G.; Bussy, F. Organization of pre-Variscan basement areas at the north-Gondwanan margin. *Int. J. Earth Sci.* **2002**, *91*, 35–52. [CrossRef]
11. Faure, M.; Lardeaux, J.M.; Ledru, P. A review of the pre-Permian geology of the Variscan French Massif Central. *Comptes Rendus Geosci.* **2009**, *341*, 202–213. [CrossRef]
12. Martín-Algarra, A.; Mazzoli, S.; Perrone, V.; Rodríguez-Cañero, R.; Navas-Parejo, P. Variscan Tectonics in the Malaguide Complex (Betic Cordillera, Southern Spain): Stratigraphic and Structural Alpine versus Pre-Alpine Constraints from the Ardales Area (Province of Malaga). I. Stratigraphy. *J. Geol.* **2009**, *117*, 241–262. [CrossRef]
13. Kroner, U.; Romer, R. Two plates—Many subduction zones: The Variscan orogeny reconsidered. *Gondwana Res.* **2013**, *24*, 298–329. [CrossRef]
14. Stampfli, G.; Hochard, C.; Vérard, C.; Wilhem, C.; von Raumer, J.F. The formation of Pangea. *Tectonophysics* **2013**, *593*, 1–19. [CrossRef]
15. Ballèvre, M.; Martínez Catalán, J.R.; ópez-Carmona, A.; Pitra, P.; Abati, J.; Fernández, R.D.; Ducassou, C.; Arenas, R.; Bosse, V.; Castiñeiras, P.; et al. *Correlation of the Nappe Stack in the Ibero-Armorican Arc across the Bay of Biscay: A Joint French–Spanish Project*; Geological Society, Special Publications: London, UK, 2014; Volume 405, pp. 77–113. [CrossRef]
16. Lardeaux, J.M. Deciphering orogeny: A metamorphic perspective Examples from European Alpine and Variscan belts: Part II: Variscan metamorphism in the French Massif Centra—A review. *Bull. Soc. Geol. Fr.* **2014**, *185*, 281–310. [CrossRef]
17. Franke, W.; Cocks, L.R.M.; Torsvik, T.H. The Palaeozoic Variscan oceans revisited. *Gondwana Res.* **2017**, *48*, 257–284. [CrossRef]
18. Martínez Catalán, J.R.; Schulmann, K.; Ghienne, J.F. The Mid-Variscan Allochthon: Keys from correlation, partial retrodeformation and plate-tectonic reconstruction to unlock the geometry of a non-cylindrical belt. *Earth-Sci. Rev.* **2021**, *220*, 103700. [CrossRef]
19. Schulmann, K.; Edel, J.B.; Martínez Catalán, J.R.; Mazur, S.; Guy, A.; Lardeaux, J.M.; Ayarza, P.; Palomeras, I. Tectonic evolution and global crustal architecture of the European Variscan belt constrained by geophysical data. *Earth-Sci. Rev.* **2022**, *234*, 104195. [CrossRef]
20. Lardeaux, J.M. Metamorphism and linked deformation in understanding tectonic processes at varied scales. *Comptes Rendus. Geosci.* **2023**, *356*, 1–25. [CrossRef]
21. von Raumer, J.F.; Neubauer, F. Late Precambrian and Palaeozoic Evolution of the Alpine Basement—An Overview. In *Pre-Mesozoic Geology in the Alps*; von Raumer, J.F., Neubauer, F., Eds.; Springer: Berlin/Heidelberg, Germany, 1993; pp. 625–639. [CrossRef]
22. von Raumer, J.F.; Stampfli, G.M.; Bussy, F. Gondwana-derived microcontinents—The constituents of the Variscan and Alpine collisional orogens. *Tectonophysics* **2003**, *365*, 7–22. [CrossRef]
23. Guillot, S.; di Paola, S.; Ménot, R.P.; Ledru, P.; Spalla, M.I.; Gosso, G.; Schwartz, S. Suture zones and importance of strike-slip faulting for Variscan geodynamic reconstructions of the External Crystalline Massifs of the western Alps. *Bull. Soc. Geol. Fr.* **2009**, *180*, 483–500. [CrossRef]
24. Compagnoni, R.; Ferrando, S.; Lombardo, B.; Radulesco, N.; Rubatto, D. Paleo-European crust of the Italian Western Alps: Geological history of the Argentera Massif and comparison with Mont Blanc-Aiguilles Rouges and Maures-Tanneron Massifs. *J. Virtual Explor.* **2010**, *36*, 228. [CrossRef]
25. Spiess, R.; Cesare, B.; Mazzoli, C.; Sassi, R.; Sassi, F.P. The crystalline basement of the Adria microplate in the eastern Alps: A review of the palaeostructural evolution from the Neoproterozoic to the Cenozoic. *Rend. Lincei* **2010**, *21*, 31–50. [CrossRef]
26. von Raumer, J.F.; Bussy, F.; Schaltegger, U.; Schulz, B.; Stampfli, G.M. Pre-Mesozoic Alpine basements-Their place in the European Paleozoic framework. *Geol. Soc. Am. Bull.* **2013**, *125*, 89–108. [CrossRef]
27. Faure, M.; Ferrière, J. Reconstructing the Variscan Terranes in the Alpine Basement: Facts and Arguments for an Alpidic Orocline. *Geosciences* **2022**, *12*, 65. [CrossRef]
28. Neubauer, F.; Liu, Y.; Dong, Y.; Chang, R.; Genser, J.; Yuan, S. Pre-Alpine tectonic evolution of the Eastern Alps: From Prototethys to Paleotethys. *Earth-Sci. Rev.* **2022**, *226*, 103923. [CrossRef]
29. Rutland, R.W.R. Andean orogeny and ocean floor spreading. *Nature* **1971**, *233*, 252–255. [CrossRef]
30. von Huene, R.; Scholl, D.W. Observations at convergent margins concerning sediment subduction, subduction erosion, and the growth of continental crust. *Rev. Geophys.* **1991**, *29*, 279–316. [CrossRef]
31. Stern, C.R. The role of subduction erosion in the generation of Andean and other convergent plate boundary arc magmas, the continental crust and mantle. *Gondwana Res.* **2020**, *88*, 220–249. [CrossRef]
32. Roda, M.; Zucali, M.; Regorda, A.; Spalla, M.I. Formation and evolution of a subduction-related mélange: The example of the Rocca Canavese Thrust Sheets (Western Alps). *GSA Bull.* **2020**, *132*, 884–896. [CrossRef]
33. Termier, P. *A la Gloire de la Terre*, 8th ed.; Desclée De Brouwer et Cie: Paris, France, 1922; p. 425.

34. Spalla, M.I.; Marotta, A.M. P-T evolutions vs. numerical modelling: A key to unravel the Paleozoic to early-Mesozoic tectonic evolution of the Alpine area. *Period. Mineral.* **2007**, *76*, 267–308. [CrossRef]
35. Regorda, A.; Lardeaux, J.M.; Roda, M.; Marotta, A.M.; Spalla, M.I. How many subductions in the Variscan orogeny? Insights from numerical models. *Geosci. Front.* **2020**, *11*, 1025–1052. [CrossRef]
36. Miyashiro, A. Evolution of Metamorphic Belts. *J. Petrol.* **1961**, *2*, 277–311. [CrossRef]
37. Ernst, W.G. Metamorphic zonations on presumably subducted lithospheric plates from Japan, California and the Alps. *Contrib. Mineral. Petrol.* **1971**, *34*, 43–59. [CrossRef]
38. Ernst, W.G. Metamorphism and Ancient Continental Margins. In *The Geology of Continental Margins*; Burk, C.A., Drake, C.L., Eds.; Springer: Berlin/Heidelberg, Germany, 1974; pp. 907–919. [CrossRef]
39. Ernst, W.G. *Petrologic Phase Equilibria*; W.H. Freeman and Co. Ltd.: San Francisco, CA, USA, 1976; p. 333.
40. Ernst, W.G. Tectonics and prograde versus retrograde P-T trajectories of High-pressure metamorphic belts. *Rend. Della Soc. Ital. Mineral. Petrol.* **1977**, *33*, 191–220.
41. England, P.C.; Richardson, S.W. The influence of erosion upon the mineral fades of rocks from different metamorphic environments. *J. Geol. Soc.* **1977**, *134*, 201–213. [CrossRef]
42. Cloos, M. Lithospheric buoyancy and collisional orogenesis: Subduction of oceanic plateaus, continental margins, island arcs, spreading ridges, and seamounts. *Geol. Soc. Am. Bull.* **1993**, *105*, 715. [CrossRef]
43. Spear, F.S. *Metamorphic Phase Equilibria and Pressure-Temperature-Time Paths*; Mineralogical Society of America: Washington, DC, USA, 1993; p. 799.
44. Kornprobst, J. *Metamorphic Rocks and Their Geodynamic Significance. Petrology and Structural Geology*, 1st ed.; Springer: Dordrecht, The Netherlands, 2002; Volume 12, p. 206. [CrossRef]
45. Royden, L.; Horváth, F.; Nagymarosy, A.; Stegena, L. Evolution of the Pannonian Basin System: 2. Subsidence and thermal history. *Tectonics* **1983**, *2*, 91–137. [CrossRef]
46. Cavazza, W.; Wezel, F.C. The Mediterranean region—A geological primer. *Episodes* **2003**, *26*, 160–168. [CrossRef]
47. Dal Piaz, G.V. The Italian Alps: A journey across two centuries of Alpine geology. *J. Virtual Explor.* **2010**, *36*, 8. [CrossRef]
48. Gosso, G.; Lardeaux, J.M.; Zanoni, D.; Volante, S.; Corsini, M.; Bersezio, R.; Mascle, J.; Spaggiari, L.; Spalla, M.I.; Zucali, M.; et al. Mapping the progressive geologic history at the junction of the Alpine Mountain Belt and the Western Mediterranean Ocean. *Ofioliti* **2019**, *44*, 97–110.
49. Polino, R.; Dal Piaz, G.V.; Gosso, G. Tectonic erosion at the Adria margin and accretionary processes for the Cretaceous orogeny of the Alps. *Mem. Soc. Geol. Fr.* **1990**, *156*, 345–367.
50. Pfiffner, A.; Lehner, P.; Heitzman, P.; Mueller, S.; Steck, A. *Deep Structure of the Swiss Alps—Results from NFP 20*; Birkhäuser: Basel, Switzerland, 1997; p. 330.
51. Schmid, S.M.; Fügenschuh, B.; Kissling, E.; Schuster, R. Tectonic map and overall architecture of the Alpine orogen. *Eclogae Geol. Helv.* **2004**, *97*, 93–117. [CrossRef]
52. Brack, P. Structures in the southwestern border of the Adamello intrusion (Alpi Bresciane, Italy). *Schweiz. Mineral. Und Petrogr. Mitteilungen* **1981**, *61*, 37–50. [CrossRef]
53. Crespi, R.; Liborio, G.; Mottana, A. Metamorfismo tardo-alpino di grado bassissimo nel basamento a sud della Linea Insubrica. *Rend. Della Soc. Ital. Mineral. Petrol.* **1981**, *37*, 813–824.
54. Filippi, M.; Zanoni, D.; Rebay, G.; Roda, M.; Regorda, A.; Lardeaux, J.M.; Spalla, M.I. Quantification of Alpine Metamorphism in the Edolo Diabase, Central Southern Alps. *Geosciences* **2022**, *12*, 312. [CrossRef]
55. Roure, F.; Heitzman, P.; Polino, R. *Deep Structure of the Alps*; Volume speciale della Società Geologica Italiana: Roma, Italy, 1990; p. 367.
56. Spalla, M.I.; Lardeaux, J.M.; Dal Piaz, G.V.; Gosso, G.; Messiga, B. Tectonic significance of Alpine eclogites. *J. Geodyn.* **1996**, *21*, 257–285. [CrossRef]
57. Handy, M.R.; Oberhänsli, R. Explanatory notes to the map: Metamorphic structure of the Alps age map of the metamorphic structure of the Alps—Tectonic interpretation and outstanding problem. *Mitt. Österr. Miner. Ges.* **2004**, *149*, 201–225.
58. Berger, A.; Bousquet, R. *Subduction-Related Metamorphism in the Alps: Review of Isotopic Ages Based on Petrology and their Geodynamic Consequences*; Geological Society Special Publications: London, UK, 2008; Volume 298, pp. 117–144. [CrossRef]
59. Platt, J.P. Dynamics of orogenic wedges and the uplift of high-pressure metamorphic rocks. *Geol. Soc. Am. Bull.* **1986**, *97*, 1037. [CrossRef]
60. Roda, M.; Spalla, M.I.; Marotta, A.M. Integration of natural data within a numerical model of ablative subduction: A possible interpretation for the Alpine dynamics of the Austroalpine crust. *J. Metamorph. Geol.* **2012**, *30*, 973–996. [CrossRef]
61. Spalla, M.I.; Zanoni, D.; Marotta, A.M.; Rebay, G.; Roda, M.; Zucali, M.; Gosso, G. *The Transition from Variscan Collision to Continental Break-Up in the Alps: Insights from the Comparison between Natural Data and Numerical Model Predictions*; Geological Society Special Publications: London, UK, 2014; Volume 405, pp. 363–400. [CrossRef]
62. Roda, M.; Regorda, A.; Spalla, M.I.; Marotta, A.M. What drives Alpine Tethys opening? Clues from the review of geological data and model predictions. *Geol. J.* **2019**, *54*, 2646–2664. [CrossRef]
63. Schulmann, K.; Catalán, J.R.M.; Lardeaux, J.M.; Janoušek, V.; Oggiano, G. The Variscan orogeny: Extent, timescale and the formation of the European crust. *Geol. Soc. Spec. Publ.* **2014**, *405*, 1–6. [CrossRef]

64. Wennekers, J. The structure of the Bergamo Alps compared with that of the North-West Highlands of Scotland. *Leidse Geol. Meded.* **1931**, *4*, 83–93.
65. de Sitter, L.U.; de Sitter-Koomans, C. The Geology of the Bergamasc Alps Lombardia Italy. *Leidse Geol. Meded.* **1949**, *14*, 1–257.
66. Gaetani, M.; Jadoul, F. The structure of Bergamasc Alps. *Atti dell'Accademia Naz. Dei Lincei* **1979**, *66*, 411–416.
67. Laubscher, H.P. Large-scale, thin-skinned thrusting in the southern Alps: Kinematic models. *Geol. Soc. Am. Bull.* **1985**, *96*, 710. [CrossRef]
68. Cassinis, G.; Dal Piaz, G.; Eusebio, A.; Gosso, G.; Martinotti, G.; Massari, F.; Milano, P.; Pennacchioni, G.; Perello, M.; Pessina, C.; et al. Report on a structural and sedimentological analysis in the Uranium Province of the Orobic Alps. *Uranium* **1986**, *2*, 241–260.
69. Milano, P.F.; Pennacchioni, G.; Spalla, M.I. Alpine and pre-Alpine tectonics in the Central Orobic Alps (Southern Alps). *Eclogae Geol. Helv.* **1988**, *81*, 273–293.
70. Carminati, E.; Siletto, G.B.; Battaglia, D. Thrust kinematics and internal deformation in basement-involved fold and thrust belts: The eastern Orobic Alps case (Central Southern Alps, northern Italy). *Tectonics* **1997**, *16*, 259–271. [CrossRef]
71. Spalla, M.I.; Gosso, G. Pre-Alpine tectonometamorphic units in the Central Southern Alps: Structural and metamorphic memory. *Mem. Sci. Geol.* **1999**, *51*, 221–229.
72. Rebay, G.; Maroni, M.; Siletto, G.B.; Spalla, M.I. Superposed syn-metamorphic structures of the Alpine and pre-Alpine convergent cycles in the Southalpine basement of the Orobic Alps (Northern Italy). *J. Maps* **2015**, *11*, 168–180. [CrossRef]
73. Zanchetta, S.; Malusà, M.G.; Zanchi, A.M. Precollisional development and Cenozoic evolution of the Southalpine retrobelt (European Alps). *Lithosphere* **2015**, *7*, L466.1. [CrossRef]
74. Ewing, T.; Hermann, J.; Rubatto, D. The robustness of the Zr-in-rutile and Ti-in-zircon thermometers during high-temperature metamorphism (Ivrea-Verbano Zone, northern Italy). *Contrib. Mineral. Petrol.* **2013**, *165*, 757–779. [CrossRef]
75. Real, C.; Fassmer, K.; Carosi, R.; Froitzheim, N.; Rubatto, D.; Groppo, C.; Münker, C.; Ferrando, S. Carboniferous-Triassic tectonic and thermal evolution of the middle crust section of the Dervio-Olgiasca Zone (Southern Alps). *J. Metamorph. Geol.* **2023**, *41*, 685–718. [CrossRef]
76. McDowell, F.W. Potassium-Argon Ages from the Ceneri Zone, Southern Swiss Alps. *Contrib. Mineral. Petrol.* **1970**, *28*, 165–182. [CrossRef]
77. di Paola, S.; Spalla, M.I.; Gosso, G. New structural mapping and metamorphic evolution of the Domaso-Cortafò Zone (Southern Alps—Lake Como). *Mem. Sci. Geol.* **2001**, *53*, 1–4.
78. Origoni Giobbi, E.; Gregnanin, A. The crystalline basement of the "Massiccio delle Tre Valli Bresciane": New petrographic and chemical data. *Mem. Della Soc. Geol. Ital.* **1983**, *26*, 133–144.
79. Riklin, K. Kontaktmetamorphose Permischer Sandsteine im Adamello-Massiv. Ph.D. Thesis, ETH Zurich, Zurich, Switzerland, 1983.
80. Spalla, M.I.; Zanoni, D.; Gosso, G.; Zucali, M. Deciphering the geologic memory of a Permian conglomerate of the Southern Alps by pebble P–T estimates. *Int. J. Earth Sci.* **2009**, *98*, 203–226. [CrossRef]
81. Filippi, M.; Spalla, M.I.; Pigazzini, N.; Diella, V.; Lardeaux, J.M.; Zanoni, D. Cld-St-And-Bearing Assemblages in the Central Southalpine Basement: Markers of an Evolving Thermal Regime during Variscan Convergence. *Minerals* **2021**, *11*, 1124. [CrossRef]
82. Zanoni, D.; Spalla, M.I.; Gosso, G. Vestiges of lost tectonic units in conglomerate pebbles? A test in Permian sequences of the Southalpine Orobic Alps. *Geol. Mag.* **2010**, *147*, 98–122. [CrossRef]
83. Zanoni, D.; Spalla, M.I. The Variscan evolution in the basement cobbles of the Permian Ponteranica Formation by microstructural and petrologic analysis. *Ital. J. Geosci.* **2018**, *137*, 254–271. [CrossRef]
84. Boriani, A.C.; Villa, I.M. Geochronology of regional metamorphism in the Ivrea-Verbano Zone and Serie dei Laghi, Italian Alps. *Schweiz. Mineral. Und Petrogr. Mitteilungen* **1997**, *77*, 381–401. [CrossRef]
85. Boriani, A.; Giobbi Origoni, E. Does the basement of western souther Alps display a tilted section through the continental crust? A review and discussion. *Period. Mineral.* **2004**, *73*, 5–22.
86. Boriani, A.; Burlini, L.; Sacchi, R. The Cossato-Mergozzo-Brissago Line and the Pogallo Line (Southern Alps, Northern Italy) and their relationships with the late-Hercynian magmatic and metamorphic events. *Tectonophysics* **1990**, *182*, 91–102. [CrossRef]
87. Borghi, A. Structural evolution of the north-eastern sector of the Serie dei Laghi (Southern Alps). *Boll. Della Soc. Geol. Ital.* **1991**, *110*, 639–647.
88. Sassi, F.; Cesare, B.; Mazzoli, C.; Peruzzo, L.; Sassi, R.; Spiess, R. The crystalline basements of the Italian Eastern Alps: A review of the metamorphic features. *Period. Mineral.* **2004**, *73*, 23–42.
89. Sassi, R.; Venturini, C.; Akrai, P. The boundary between the metamorphic and non- to anchi-metamorphic domains in the Southalpine basement s.l. of the eastern southern Alps: A review. *Period. Mineral.* **2004**, *73*, 131–143.
90. von Raumer, J. The Palaeozoic evolution in the Alps: From Gondwana to Pangea. *Geol. Rundsch.* **1998**, *87*, 407–435. [CrossRef]
91. Desmons, J.; Compagnoni, R.; Cortesogno, L.; Frey, M.; Gaggero, L. Pre-Alpine metamorphism of the internal zone of the Western Alps. *Schweiz. Mineral. Und Petrogr. Mitteilungen* **1999**, *79*, 23–39.
92. Miller, C.; Thöni, M. Origin of eclogites from the Austroalpine Ötztal basement (Tirol, Austria): Geochemistry and Sm-Nd vs. Rb-Sr isotope systematics. *Chem. Geol.* **1995**, *122*, 199–225. [CrossRef]
93. Gosso, G.; Spalla, M.I.; Messiga, B. Dumorterite-Kyanite relicts within the HT-LP country rocks of the Sondalo gabbro: A record of extension related to uplift of HP-rocks. In Proceedings of the IOS International Ophiolite Symposium, Pavia, Italy, 18–23 September 1995; p. 55.

94. Godard, G.; Martin, S.; Prosser, G.; Kienast, J.; Morten, L. Variscan migmatites, eclogites and garnet-peridotites of the Ulten zone, Eastern Austroalpine system. *Tectonophysics* **1996**, *259*, 313–341. [CrossRef]
95. Zucali, M. La Correlazione nei Terreni Metamorfici: Due Esempi dall'Austroalpino Occidentale (Zona Sesia-Lanzo) e Centrale (Falda Languard-Campo/Serie del Tonale). Ph.D. Thesis, Università degli Studi di Milano, Milano, Italy, 2001.
96. Morten, L.; Nimis, P.; Rampone, E. Records of mantle–crust exchange processes during continental subduction–exhumation in the Nonsberg–Ultental garnet peridotites (eastern Alps). A review. *Period. Mineral.* **2004**, *73*, 119–129.
97. Konzett, J.; Miller, C.; Armstrong, R.; Thöni, M. Metamorphic Evolution of Iron-rich Mafic Cumulates from the Oeztal-Stubai Crystalline Complex, Eastern Alps, Austria. *J. Petrol.* **2004**, *46*, 717–747. [CrossRef]
98. Roda, M.; Zucali, M.; Li, Z.X.; Spalla, M.I.; Yao, W. Pre-Alpine contrasting tectono-metamorphic evolutions within the Southern Steep Belt, Central Alps. *Lithos* **2018**, *310–311*, 31–49. [CrossRef]
99. Schweinehage, R.; Massone, H.J. Geochemistry and metamorphic evolution of metabasites from Silvretta nappe, Eastern Alps. *Mem. Sci. Geol.* **1999**, *51*, 191–203.
100. Andreatta, C. La formazione gneissico-kinzigitica e le oliviniti di Val d'Ultimo (Alto Adige). *Mem. Mus. Stor. Natturale Venezia Tridentina* **1935**, *3*, 1–160.
101. Herzberg, C.; Riccio, L.; Chiesa, S.; Fornoni, A.; Gatto, G.O.; Gregnanin, A.; Piccrillo, E.M.; Scolari. Petrogenetic evolution of a spinel-garnet-lherzolite in the Austridic crystalline basement from Val di Clapa. *Cons. Naz. Delle Ric. Mem. dell'Instituto Geol. Mineral. Padova* **1977**, *30*, 3–28.
102. Tumiati, S.; Thöni, M.; Nimis, P.; Martin, S.; Mair, V. Mantle–crust interactions during Variscan subduction in the Eastern Alps (Nonsberg–Ulten zone): Geochronology and new petrological constraints. *Earth Planet. Sci. Lett.* **2003**, *210*, 509–526. [CrossRef]
103. Thélin, P.; Sartori, M.; Burri, M.; Gouffon, Y.; Chessex, R. The Pre-Alpine Basement of the Briançonnais (Wallis, Switzerland). In *Pre-Mesozoic Geology in the Alps*; von Raumer, J., Neubauer, F., Eds.; Springer: Berlin/Heidelberg, Germany, 1993; pp. 297–315. [CrossRef]
104. Desmons, J.; Mercier, D. Passing through the Briançon zone. In *Pre-Mesozoic Geology in the Alp*; von Raumer, J., Neubauer, F., Eds.; Springer: Berlin/Heidelberg, Germany, 1993; pp. 279–296.
105. Boriani, A.; Dal Piaz, G.; Hunziker, J.; von Raumer, J.F.; Sassi, F. Caratteri, distribuzione ed età del metamorfismo pre-Alpino nelle Alpi. *Mem. Della Soc. Geol. Ital.* **1974**, *13*, 165–225.
106. Frisch, W.; Ménot, R.P.; Neubauer, F.; von Raumer, J. Correlation and evolution of the Alpine basement. *Schweiz. Mineral. Und Petrogr. Mitteilungen* **1990**, *70*, 265–285.
107. Dal Piaz, G. Evolution of Austro-Alpine and Upper Penninic Basement in the Northwestern Alps from Variscan Convergence to Post-Variscan Extension. In *Pre-Mesozoic Geology in the Alps*; Raumer, J.F., Neubauer, F., Eds.; Springer: Berlin/Heidelberg, Germany, 1993; pp. 327–344. [CrossRef]
108. Bergomi, M.A.; Dal Piaz, G.; Malusà, M.G.; Monopoli, B.; Tunesi, A. The Grand St Bernard-Briançonnais Nappe System and the Paleozoic Inheritance of the Western Alps Unraveled by Zircon U-Pb Dating. *Tectonics* **2017**, *36*, 2950–2972. [CrossRef]
109. Thélin, P.; Sartori, M.; Lengeler, R.; Schaerer, J.P. Eclogites of Paleozoic or early Alpine age in the basement of the Penninic Siviez-Mischabel nappe, Wallis, Switzerland. *Lithos* **1990**, *25*, 71–88. [CrossRef]
110. Bussy, F.; Sartori, M.; Thélin, P. U-Pb zircon dating in the middle Penninic basement of the Western Alps (Valais, Switzerland). *Schweiz. Mineral. Und Petrogr. Mitteilungen* **1996**, *76*, 81–84. [CrossRef]
111. Borghi, A.; Gattiglio, M.; Mondino, F.; Zaccone, G. Structural and metamorphic evidence of pre-Alpine basement in the Ambin nappe (Cottian Alps, Italy). *Mem. Della Soc. Geol. Ital.* **1999**, *51*, 205–220.
112. Giorgis, D.; Thélin, P.; Stampfli, G.M.; Bussy, F. The Mont-Mort metapelites: Variscan metamorphism and geodynamic context (Briançonnais basement, Western Alps, Swizerland). *Schweiz. Mineral. Und Petrogr. Mitteilungen* **1999**, *79*, 381–398. [CrossRef]
113. Droop, G.T.R. Pre-Alpine eclogites in the Pennine Basement Complex of the Eastern Alps. *J. Metamorph. Geol.* **1983**, *1*, 3–12. [CrossRef]
114. Zimmermann, V.R.; Franz, G. Die eklogite der Unteren schieferhülle; Frosnitztal/Südvenediger (Tauern, Oesterreich). *Mittelungen Der Oestereichischen Geol. Ges.* **1989**, *81*, 167–188.
115. Droop, G.T.R.; Lombardo, B.; Pognante, U. Formation and distribution of eclogite facies rocks in the Alps. In *Eclogite Facies Rocks*; Carswell, D.A., Ed.; Blackie: Glasgow, UK, 1990; pp. 225–259.
116. Messiga, B.; Tribuzio, R.; Caucia, F. Amphibole evolution in Variscan eclogite-amphibolites from the Savona crystalline massif (Western Ligurian Alps, Italy): Controls on the decompressional P-T-t path. *Lithos* **1991**, *27*, 215–230.
117. von Quadt, A.; Günther, D.; Frischknecht, R. The evolution of pre-Variscan ecloogites of the Tauern Window (Eastern Alps): A Sm/Nd-, conventional and Laser ICP-MS zircon U-Pb study. *Schweiz. Mineral. Und Petrogr. Mitteilungen* **1997**, *77*, 265–279. [CrossRef]
118. Nussbaum, C.; Marquer, D.; Biino, G.G. Two subduction events in a polycyclic basement: Alpine and pre-Alpine high-pressure metamorphism in the Suretta nappe, Swiss Eastern Alps. *J. Metamorph. Geol.* **1998**, *16*, 591–605. [CrossRef]
119. Dale, J.; Holland, T.J.B. Geothermobarometry, P-T paths and metamorphic field gradients of high-pressure rocks from the Adula Nappe, Central Alps. *J. Metamorph. Geol.* **2003**, *21*, 813–829. [CrossRef]
120. Giacomini, F.; Braga, R.; Tiepolo, M.; Tribuzio, R. New constraints on the origin and age of Variscan eclogitic rocks (Ligurian Alps, Italy). *Contrib. Mineral. Petrol.* **2007**, *153*, 29–53. [CrossRef]

121. Liati, A.; Gebauer, D.; Fanning, C. Geochronological evolution of HP metamorphic rocks of the Adula nappe, Central Alps, in pre-Alpine and Alpine subduction cycles. *J. Geol. Soc.* **2009**, *166*, 797–810. [CrossRef]
122. Maino, M.; Dallagiovanna, G.; Gaggero, L.; Seno, S.; Tiepolo, M. U-Pb zircon geochronological and petrographic constraints on late to post-collisional Variscan magmatism and metamorphism in the Ligurian Alps, Italy. *Geol. J.* **2012**, *47*, 632–652. [CrossRef]
123. Schaltegger, U. Unravelling the pre-Mesozoic history of Aar and Gotthard massifs (Central Alps) by isotopic dating: A review. *Schweiz. Mineral. Petrogr. Mitteilungen* **1994**, *74*, 41–51. [CrossRef]
124. von Raumer, J.; Abrecht, J.; Bussy, F.; Lombardo, B.; Ménot, R.; Schaltegger, U. The Paleozoic metamorphic evolution of the Alpine External Massifs. *Schweiz. Mineral. Petrogr. Mitteilungen* **1999**, *79*, 5–22.
125. von Raumer, J.; Bussy, F. Mont Blanc and Aiguilles-Rouges: Geology of their polymetamorphic basement (External massifs, France- Switzerland). *Mem. Geol. Lausanne* **2004**, *42*, 1–203.
126. Jacob, J.; Guillot, S.; Rubatto, D.; Janots, E.; Melleton, J.; Faure, M. Carboniferous high-P metamorphism and deformation in the Belledonne Massif (Western Alps). *J. Metamorph. Geol.* **2021**, *39*, 1009–1044. [CrossRef]
127. Vanardois, J.; Roger, F.; Trap, P.; Goncalves, P.; Lanari, P.; Paquette, J.; Marquer, D.; Cagnard, F.; Le Bayon, B.; Melleton, J.; et al. Exhumation of deep continental crust in a transpressive regime: The example of Variscan eclogites from the Aiguilles-Rouges massif (Western Alps). *J. Metamorph. Geol.* **2022**, *40*, 1087–1120. [CrossRef]
128. Corsini, M.; Ruffet, G.; Caby, R. Alpine and late-hercynian geochronological constraints in the Argentera Massif (Western Alps). *Eclogae Geol. Helv.* **2004**, *97*, 3–15. [CrossRef]
129. Sanchez, G.; Rolland, Y.; Schneider, J.; Corsini, M.; Oliot, E.; Goncalves, P.; Verati, C.; Lardeaux, J.M.; Marquer, D. Dating low-temperature deformation by $^{40}Ar/^{39}Ar$ on white mica, insights from the Argentera-Mercantour Massif (SW Alps). *Lithos* **2011**, *125*, 521–536. [CrossRef]
130. Filippi, M.; Zanoni, D.; Gosso, G.; Lardeaux, J.M.; Verati, C.; Spalla, M.I. Structure of lamprophyres: A discriminant marker for Variscan and Alpine tectonics in the Argentera-Mercantour Massif, Maritime Alps. *BSGF—Earth Sci. Bull.* **2019**, *190*, 12. [CrossRef]
131. Filippi, M.; Zanoni, D.; Lardeaux, J.M.; Spalla, M.I.; Gosso, G. Evidence of Tethyan continental break-up and Alpine collision in the Argentera-Mercantour Massif, Western Alps. *Lithos* **2020**, *372–373*, 105653. [CrossRef]
132. von Raumer, J.F. Zur Metamorphose amphibolitischer Gesteine im Altkristallin des Mont-Blanc- und Aguilles-Rouges-Massivs. *Schweiz. Mineral. Und Petrogr. Mitteilungen* **1974**, *54*, 471–488.
133. Liégeois, J.P.; Duchesne, J.C. The Lac Cornu retrograded eclogites (Aiguilles Rouges massif, Western Alps, France): Evidence of crustal origin and metasomatic alteration. *Lithos* **1981**, *14*, 35–48. [CrossRef]
134. Latouche, L.; Bogdanoff, S. Evolution précoce du massif de l'Argentera: Apport des eclogites et des granulites; Les massifs cristallins externs. *Geol. Alp.* **1987**, *63*, 151–164.
135. Bogdanoff, S.; Ménot, R.; Vivier, G. Les massif cristallins externes des Alpes occidentales françaises, un fragment de la zone interne varisque. *Sci. Geol. Bull.* **1991**, *44*, 237–285. [CrossRef]
136. Colombo, F.; Compagnoni, R.; Lombardo, B. Le rocce eclogitiche dei Laghi del Frisson (Argentera sud-orientale, Alpi Marittime). *Atti Ticinesi Sci. Della Terra Ser. Spec.* **1994**, *1*, 75–82.
137. Ferrando, S.; Lombardo, B.; Compagnoni, R. Metamorphic history of HP mafic granulites from the Gesso-Stura Terrain (Argentera Massif, Western Alps, Italy). *Eur. J. Mineral.* **2008**, *20*, 777–790. [CrossRef]
138. Jouffray, F.; Spalla, M.I.; Lardeaux, J.M.; Filippi, M.; Rebay, G.; Corsini, M.; Zanoni, D.; Zucali, M.; Gosso, G. Variscan eclogites from the Argentera-Mercantour Massif (External Crystalline Massifs, SW Alps): A dismembered cryptic suture zone. *Int. J. Earth Sci.* **2020**, *109*, 1273–1294. [CrossRef]
139. Paquette, J.L.; Ballèvre, M.; Peucat, J.J.; Cornen, G. From opening to subduction of an oceanic domain constrained by LA-ICP-MS U-Pb zircon dating (Variscan belt, Southern Armorican Massif, France). *Lithos* **2017**, *294–295*, 418–437. [CrossRef]
140. Zucali, M.; Corti, L.; Roda, M.; Ortolano, G.; Visalli, R.; Zanoni, D. Quantitative X-ray Maps Analaysis of Composition and Microstructure of Permian High-Temperature Relicts in Acidic Rocks from the Sesia-Lanzo Zone Eclogitic Continental Crust, Western Alps. *Minerals* **2021**, *11*, 1421. [CrossRef]
141. Whitney, D.L.; Evans, B.W. Abbreviations for names of rock-forming minerals. *Am. Mineral.* **2010**, *95*, 185–187. [CrossRef]
142. Boriani, A.; Giobbi Mancini, E.; Villa, I. Pre-Alpine ophiolites in the basement of Southern Alps: The presence of a bimodal association (LAG- Leptyno-Amphibolitic Group) in the Serie del Laghi (N-Italy, Ticino-CH). *Rend. Lincei* **2003**, *14*, 79–101. [CrossRef]
143. Fumasoli, M. Geologie des Gebietes Nördlich und Südlich der Jorio-Tonale-Linie im Westen von Gravedona (Como, Italia). Ph.D. Thesis, ETH—Zurich, Zurich, Switzerland, 1974.
144. di Paola, S.; Spalla, M.I. Contrasting tectonic records in pre-Alpine metabasites of the Southern Alps (lake Como, Italy). *J. Geodyn.* **2000**, *30*, 167–189. [CrossRef]
145. Bocchio, R.; De Capitani, L.; Liborio, G.; Mottana, A.; Nicoletti, M.; Petrucciani, C. K-Ar radiometric age determinations of the South-Alpine metamorphic complex, western Orobic Alps (Italy). *Neues Jahrb. Fur Mineral.—Monatshefte* **1981**, *7*, 289–307.
146. Mottana, A.; Nicoletti, M.; Petrucciani, C.; Liborio, G.; De Capitani, L.; Bocchio, R. Pre-alpine and alpine evolution of the South-alpine basement of the Orobic Alps. *Geol. Rundsch.* **1985**, *74*, 353–366. [CrossRef]
147. Bertotti, G.; Siletto, G.; Spalla, M. Deformation and metamorphism associated with crustal rifting: The Permian to Liassic evolution of the Lake Lugano-Lake Como area (Southern Alps). *Tectonophysics* **1993**, *226*, 271–284. [CrossRef]

148. Siletto, G.B.; Spalla, M.I.; Tunesi, A.; Lardeaux, J.M.; Colombo, A. Pre-Alpine Structural and Metamorphic Histories in the Orobic Southern Alps, Italy. In *Pre-Mesozoic Geology in the Alps*; Springer: Berlin/Heidelberg, Germany, 1993; pp. 585–598. [CrossRef]
149. Diella, V.; Spalla, M.I.; Tunesi, A. Contrasting thermomechanical evolutions in the Southalpine metamorphic basement of the Orobic Alps (Central Alps, Italy). *J. Metamorph. Geol.* **1992**, *10*, 203–219. [CrossRef]
150. Spalla, M.I.; Carminati, E.; Ceriani, S.; Oliva, A.; Battaglia, D. Influence of deformation partitioning and metamorphic re-equilibration on P-T path reconstruction in the pre-Alpine basement of central Southern Alps (Northern Italy). *J. Metamorph. Geol.* **2001**, *17*, 319–336. [CrossRef]
151. Benciolini, L.; Poli, M.E.; Visonà, D.; Zanferrari, A. Looking inside Late Variscan tectonics: Structural and metamorphic heterogeneity of the Eastern Southalpine Basement (NE Italy). *Geodin. Acta* **2006**, *19*, 17–32. [CrossRef]
152. Zucali, M.; Manzotti, P.; Diella, V.; Pesenti, C.; Risplendente, A.; Darling, J.; Engi, M. Permian tectonometamorphic evolution of the Dent-Blanche Unit (Austroalpine domain, Western Italian Alps). *Rend. Online Della Soc. Geol. Ital.* **2011**, *15*, 133–136.
153. Manzotti, P.; Zucali, M. The pre-Alpine tectonic history of the Austroalpine continental basement in the Valpelline unit (Western Italian Alps). *Geol. Mag.* **2013**, *150*, 153–172. [CrossRef]
154. Kunz, B.E.; Manzotti, P.; von Niederhäusern, B.; Engi, M.; Darling, J.R.; Giuntoli, F.; Lanari, P. Permian high-temperature metamorphism in the Western Alps (NW Italy). *Int. J. Earth Sci.* **2018**, *107*, 203–229. [CrossRef]
155. Gardien, V.; Reusser, E.; Marquer, D. Pre-Alpine metamorphic evolution of the gneisses from the Valpelline series (Western Alps, Italy). *Schweiz. Mineral. Und Petrogr. Mitteilungen* **1994**, *74*, 489–502. [CrossRef]
156. Maggetti, M.; Galetti, G. Evolution of the Silvretta eclogites: Metamorphic and magmatic events. *Schweiz. Mineral. Petrogr. Mitteilungen* **1988**, *68*, 467–484. [CrossRef]
157. Maggetti, M.; Flisch, M. Evolution of the Silvretta Nappe. In *Pre-Mesozoic Geology in the Alps*; von Raumer, J.F., Neubauer, F., Eds.; Springer: Berlin/Heidelberg, Germany, 1993; pp. 469–484. [CrossRef]
158. Melcher, F.; Meisel, T.; Puhl, J.; Koller, F. Petrogenesis and geotectonic setting of ultramafic rocks in the Eastern Alps: Constraints from geochemistry. *Lithos* **2002**, *65*, 69–112. [CrossRef]
159. Ladenhauf, C.; Armstrong, R.; Konzett, J.; Miller, C. The timing of pre-Alpine high-pressure metamorphism in the Eastern Alps: Constraints from U–Pb SHRIMP dating of eclogite zircons from the Austroalpine Silvretta nappe. *J. Conf. Abstr.* **2001**, *6*, 600.
160. Brugger, J. Les veines à andalousite du Pischahorn (Grisons, Suisse) = Andalusite veins from the Pischahorn (Grisons, Switzerland). *Schweiz. Mineral. Und Petrogr. Mitteilungen* **1994**, *74*, 191–202. [CrossRef]
161. Giacomini, F.; Messiga, B.; Tribuzio, R.; Braga, R. The Sondalo gabbroic complex and its country rocks: New geological and petrological data. In *Tuebinger Geowissenschaftliche Arbeiten. Reihe A: Geologie, Palaeontologie, Stratigraphie*; Institut für Geowissenschaften: Kiel, Germany, 1999; p. 156.
162. Tribuzio, R.; Thirwall, M.F.; Messiga, B. Petrology, mineral and isotope geochemistry of the Sondalo gabbroic complex (Central Alps, Northern Italy): Implications for the origin of post-Variscan magmatism. *Contrib. Mineral. Petrol.* **1999**, *136*, 48–62. [CrossRef]
163. Petri, B.; Mohn, G.; Štípská, P.; Schulmann, K.; Manatschal, G. The Sondalo gabbro contact aureole (Campo unit, Eastern Alps): Implications for mid-crustal mafic magma emplacement. *Contrib. Mineral. Petrol.* **2016**, *171*, 52. [CrossRef]
164. Gregnanin, A. Metamorphism and magmatism in the western italian Tyrol. *Riv. Ital. Mineral. Petrol.* **1980**, *36*, 49–64.
165. Haas, R. Zur Metamorphose des Suedlichen Oetz—Talkristallins unter Besonderer Beruecksichtigung der Matscher Einheit (Vintschgau/Suedtirol). Ph.D. Thesis, University of Innsbruck, Innsbruck, Austria, 1985.
166. Thöni, M. Sm–Nd isotope systematics in garnet from different lithologies (Eastern Alps): Age results, and an evaluation of potential problems for garnet Sm–Nd chronometry. *Chem. Geol.* **2002**, *185*, 255–281. [CrossRef]
167. Rode, S.; Rösel, D.; Schulz, B. Constraints on the Variscan P-T evolution by EMP Th-U-Pb monazite dating in the polymetamorphic Austroalpine Oetztal-Stubai basement (Eastern Alps). *Z. Der Dtsch. Ges. Fur Geowiss.* **2012**, *163*, 43–67. [CrossRef]
168. Thöny, W.F.; Tropper, P.; Schennach, F.; Krenn, E.; Finger, F.; Kaindl, R.; Bernhard, F.; Hoinkes, G. The metamorphic evolution of migmatites from the Ötztal Complex (Tyrol, Austria) and constraints on the timing of the pre-Variscan high-T event in the Eastern Alps. *Swiss J. Geosci.* **2008**, *101*, 111–126. [CrossRef]
169. Hoinkes, G.; Thöni, M.; Lichem, C. Metagranitoids and associated metasediments as indicators for the pre-Alpine magmatic and metamorphic evolution of the western Austroalpine Ötztal Basement (Kaunertal, Tirol). *Schweiz. Mineral. Und Petrogr. Mitteilungen* **1997**, *77*, 299–314.
170. Schulz, B.; Krause, J.; Zimmermann, R. Electron microprobe petrochronology of monazite-bearing garnet micaschists in the Oetztal-Stubai Complex (Alpeiner Valley, Stubai). *Swiss J. Geosci.* **2019**, *112*, 597–617. [CrossRef]
171. Hauzenberger, C.; Höller, W.; Hoinkes, G.; Kloetzli, U.; Thöni, M. Metamorphic evolution of the Austroalpine basement in the Nonsberg area, Ultental (Val d'Ultimo), Southern Tyrol. *Terra Nova* **1993**, *5*, 13.
172. Hauzenberger, C.A.; Höller, W.; Hoinkes, G. Transition from eclogite to amphibolite-facies metamorphism in the Austroalpine Ulten Zone. *Mineral. Petrol.* **1996**, *58*, 111–130. [CrossRef]
173. Braga, R.; Massonne, H.J.; Morten, L. An early metamorphic stage for the Variscan Ulten Zone gneiss (NE Italy): Evidence from mineral inclusions in kyanite. *Mineral. Mag.* **2007**, *71*, 691–702. [CrossRef]
174. Langone, A.; Braga, R.; Massonne, H.J.; Tiepolo, M. Preservation of old (prograde metamorphic) U-Th-Pb ages in unshielded monazite from the high-pressure paragneisses of the Variscan Ulten Zone (Italy). *Lithos* **2011**, *127*, 68–85. [CrossRef]

175. Tumiati, S.; Godard, G.; Martin, S.; Klötzli, U.; Monticelli, D. Fluid-controlled crustal metasomatism within a high-pressure subducted mélange (Mt. Hochwart, Eastern Italian Alps). *Lithos* **2007**, *94*, 148–167. [CrossRef]
176. Krenn, E.; Schulz, B.; Finger, F. Three generations of monazite in Austroalpine basement rocks to the south of the Tauern Window: Evidence for Variscan, Permian and Eo-Alpine metamorphic events. *Swiss J. Geosci.* **2012**, *105*, 343–360. [CrossRef]
177. Hauke, M.; Froitzheim, N.; Nagel, T.J.; Miladinova, I.; Fassmer, K.; Fonseca, R.O.C.; Sprung, P.; Münker, C. Two high-pressure metamorphic events, Variscan and Alpine, dated by Lu–Hf in an eclogite complex of the Austroalpine nappes (Schobergruppe, Austria). *Int. J. Earth Sci.* **2019**, *108*, 1317–1331. [CrossRef]
178. Faryad, S.W.; Melcher, F.; Hoinkes, G.; Puhl, J.; Meisel, T.; Frank, W. Relics of eclogite facies metamorphism in the Austroalpine basement, Hochgroessen (Speik complex), Austria. *Mineral. Petrol.* **2002**, *74*, 49–73.
179. Faryad, S.W.; Hoinkes, G. P-T gradient of Eo-Alpine metamorphism within the Austroalpine basement units east of the Tauern Window (Austria). *Mineral. Petrol.* **2003**, *77*, 129–159. [CrossRef]
180. Schermaier, A.; Haunschmid, B.; Finger, F. Distribution of Variscan I- and S-type granites in the Eastern Alps: A possible clue to unravel pre-Alpine basement structures. *Tectonophysics* **1997**, *272*, 315–333. [CrossRef]
181. Schulz, B. Polymetamorphism in garnet micaschists of the Saualpe Eclogite Unit (Eastern Alps, Austria), resolved by automated SEM methods and EMP-Th-U-Pb monazite dating. *J. Metamorph. Geol.* **2017**, *35*, 141–163. [CrossRef]
182. Nagy, G.; Draganits, E.; Demény, A.; Pantó, G.; Árkai, P. Genesis and transformations of monazite, florencite and rhabdophane during medium grade metamorphism: Examples from the Sopron Hills, Eastern Alps. *Chem. Geol.* **2002**, *191*, 25–46. [CrossRef]
183. Monié, P. Preservation of Hercynian $^{40}Ar/^{39}Ar$ ages through high-pressure low-temperature Alpine metamorphism in the Western Alps. *Eur. J. Mineral.* **1990**, *2*, 343–361. [CrossRef]
184. Nosenzo, F.; Manzotti, P.; Poujol, M.; Ballèvre, M.; Langlade, J. A window into an older orogenic cycle: P-T conditions and timing of the pre-Alpine history of the Dora-Maira Massif (Western Alps). *J. Metamorph. Geol.* **2022**, *40*, 789–821. [CrossRef]
185. Le Bayon, B.; Pitra, P.; Ballèvre, M.; Bohn, M. Reconstructing P-T paths during continental collision using multi-stage garnet (Gran Paradiso nappe, Western Alps). *J. Metamorph. Geol.* **2006**, *24*, 477–496. [CrossRef]
186. Gasco, I.; Gattiglio, M. Geological map of the middle Orco Valley, Western Italian Alps. *J. Maps* **2011**, *7*, 463–477. [CrossRef]
187. Rubatto, D.; Ferrando, S.; Compagnoni, R.; Lombardo, B. Carboniferous high-pressure metamorphism of Ordovician protoliths in the Argentera Massif (Italy), Southern European Variscan belt. *Lithos* **2010**, *116*, 65–76. [CrossRef]
188. Le Fort, P. Geologie du Haut-Dauphine Cristallin (Alpes Française): Etudes Petrologique et Structurale de la Partie Occidentale. Ph.D. Thesis, Université Nancy, Nancy, France, 1973.
189. Guillot, S.; Ménot, R.P.; Fernandez, A. Paleozoic evolution of the external crystalline massifs along the Belledonne-Oisans transect (Western Alps). *Acta Univ. Carol. Geol.* **1998**, *42*, 257–258.
190. Grandjean, V.; Guillot, S.; Pecher, A. A new record of the LP-HT late-Variscan metamorphism: The Peyre-Arguet unit (Haut-Dauphiné). *Comptes Rendus L'Academie Des Science Serie 2, Fascicule Sciences Terre Des Planetes: Earth Planet* **1996**, *322*, 189–195.
191. Jacob, J.B.; Janots, E.; Guillot, S.; Rubatto, D.; Fréville, K.; Melleton, J.; Faure, M. HT overprint of HP granulites in the Oisans–Pelvoux massif: Implications for the dynamics of the Variscan collision in the external western Alps. *Lithos* **2022**, *416–417*, 106650. [CrossRef]
192. Jacob, J.B.; Janots, E.; Cordier, C.; Guillot, S. Discovery of Variscan orogenic peridotites in the Pelvoux Massif (Western Alps, France). *BSGF—Earth Sci. Bull.* **2023**, *194*, 2. [CrossRef]
193. di Paola, S. Eredità Litostratigrafica, Strutturale e Metamorfica Paleozoica nel Margine Interno Europeo (Grandes Rousses e Argentera), Ristrutturato Durante l'Orogenesi Alpina. Ph.D. Thesis, Università degli Studi di Milano, Milano, Italy, 2001.
194. Guillot, S.; Ménot, R.P. Nappe stacking and first evidence of Late Variscan extension in the Belledonne Massif (External Crystalline Massifs, French Alps). *Geodin. Acta* **1999**, *12*, 97–111. [CrossRef]
195. Ménot, R.P.; Bonhomme, M.G.; Vivier, G. Structuration tectono-métamorphique carbonifère dans le massif de Belledonne (Alpes occidentales françaises): Apport de la géochronologie K/Ar des amphiboles. *Schweiz. Mineral. Und Petrogr. Mitteilungen* **1987**, *67*, 273–284. [CrossRef]
196. Fréville, K.; Trap, P.; Faure, M.; Melleton, J.; Li, X.H.; Lin, W.; Blein, O.; Bruguier, O.; Poujol, M. Structural, metamorphic and geochronological insights on the Variscan evolution of the Alpine basement in the Belledonne Massif (France). *Tectonophysics* **2018**, *726*, 14–42. [CrossRef]
197. Schulz, B.; von Raumer, J.F. Discovery of Ordovician–Silurian metamorphic monazite in garnet metapelites of the Alpine External Aiguilles Rouges Massif. *Swiss J. Geosci.* **2011**, *104*, 67–79. [CrossRef]
198. Genier, F.; Bussy, F.; Epard, J.L.; Baumgartner, L. Water-assisted migmatization of metagraywackes in a Variscan shear zone, Aiguilles-Rouges massif, western Alps. *Lithos* **2008**, *102*, 575–597. [CrossRef]
199. Bussy, F.; Hernandez, J.; von Raumer, J.F. Bimodal magmatism as a consequence of the post-collisional readjustment of the thickened variscan continental lithosphere (Aiguilles Rouges/Mont-Blanc massifs, western Alps). *Trans. R. Soc. Edinb.* **2000**, *91*, 221–233.
200. Dobmeier, C. Variscan P-T deformation paths from the southwestern Aiguilles Rouges massif (External massif, western Alps) and their implication for its tectonic evolution. *Geologische Rundschau* **1998**, *87*, 107–123. [CrossRef]
201. Marshall, D.; Kirschner, D.; Bussy, F. A Variscan pressure-temperature-time path for the N-E Mont Blanc massif. *Contrib. Mineral. Petrol.* **1997**, *126*, 416–428. [CrossRef]

202. Schaltegger, U. The evolution of the polymetamorphic basement in the Central Alps unravelled by precise U-Pb zircon dating. *Contrib. Mineral. Petrol.* **1993**, *113*, 466–478. [CrossRef]
203. Paquette, J.L.; Ménot, R.P.; Peucat, J.J. REE, SmNd and UPb zircon study of eclogites from the Alpine External Massifs (Western Alps): Evidence for crustal contamination. *Earth Planet. Sci. Lett.* **1989**, *96*, 181–198. [CrossRef]
204. Ernst, W.G.; Liou, J.G. High- and ultrahigh-pressure metamorphism: Past results and future prospects. *Am. Mineral.* **2008**, *93*, 1771–1786. [CrossRef]
205. Regorda, A.; Spalla, M.I.; Roda, M.; Lardeaux, J.; Marotta, A.M. Metamorphic Facies and Deformation Fabrics Diagnostic of Subduction: Insights From 2D Numerical Models. *Geochem. Geophys. Geosyst.* **2021**, *22*, e2021GC009899. [CrossRef]
206. Gasco, I.; Borghi, A.; Gattiglio, M. Metamorphic evolution of the Gran Paradiso Massif: A case study of an eclogitic metagabbro and a polymetamorphic glaucophane–garnet micaschist. *Lithos* **2010**, *115*, 101–120. [CrossRef]
207. Ernst, W.G. Interpretative Synthesis of Metamorphism in the Alps. *Geol. Soc. Am. Bull.* **1973**, *84*, 2053. [CrossRef]
208. England, P.C.; Thompson, A.B. Pressure–Temperature–Time Paths of Regional Metamorphism I. Heat Transfer during the Evolution of Regions of Thickened Continental Crust. *J. Petrol.* **1984**, *25*, 894–928. [CrossRef]
209. Thompson, A.B.; England, P.C. Pressure–Temperature–Time Paths of Regional Metamorphism II. Their Inference and Interpretation using Mineral Assemblages in Metamorphic Rocks. *J. Petrol.* **1984**, *25*, 929–955. [CrossRef]
210. Jamieson, R.A.; Beaumont, C.; Fullsack, P.; Lee, B. *Barrovian Regional Metamorphism: Where's the Heat?* Geological Society Special Publication: London, UK, 1998; Volume 138, pp. 23–51. [CrossRef]
211. Sandiford, M.; Powell, R. Some remarks on high-temperature-low-pressure metamorphism in convergent orogens. *J. Metamorph. Geol.* **1991**, *9*, 333–340. [CrossRef]
212. Ryan, P.D.; Dewey, J.F. The sources of metamorphic heat during collisional orogeny: The Barrovian enigma. *Can. J. Earth Sci.* **2019**, *56*, 1309–1317. [CrossRef]
213. Mevel, C.; Caby, R.; Kienast, J.R. Amphibolite facies conditions in the oceanic crust: Example of amphibolitized flaser-gabbro and amphibolites from the Chenaillet ophiolite massif (Hautes Alpes, France). *Earth Planet. Sci. Lett.* **1978**, *39*, 98–108. [CrossRef]
214. Verati, C.; Lardeaux, J.M.; Favier, A.; Corsini, M.; Philippon, M.; Legendre, L. Arc-related metamorphism in the Guadeloupe archipelago (Lesser Antilles active island arc): First report and consequences. *Lithos* **2018**, *320–321*, 592–598. [CrossRef]
215. Vanderhaeghe, O. The thermal–mechanical evolution of crustal orogenic belts at convergent plate boundaries: A reappraisal of the orogenic cycle. *J. Geodyn.* **2012**, *56–57*, 124–145. [CrossRef]
216. Penniston-Dorland, S.C.; Kohn, M.J.; Manning, C.E. The global range of subduction zone thermal structures from exhumed blueschists and eclogites: Rocks are hotter than models. *Earth Planet. Sci. Lett.* **2015**, *428*, 243–254. [CrossRef]
217. Lotout, C.; Pitra, P.; Poujol, M.; Anczkiewicz, R.; Van Den Driessche, J. Timing and duration of Variscan high-pressure metamorphism in the French Massif Central: A multimethod geochronological study from the Najac Massif. *Lithos* **2018**, *308–309*, 381–394. [CrossRef]
218. Lotout, C.; Poujol, M.; Pitra, P.; Anczkiewicz, R.; Van Den Driessche, J. From Burial to Exhumation: Emplacement and Metamorphism of Mafic Eclogitic Terranes Constrained Through Multimethod Petrochronology, Case Study from theévézou Massif (French Massif Central, Variscan Belt). *J. Petrol.* **2020**, *61*, egaa046. [CrossRef]
219. Pitra, P.; Poujol, M.; Van Den Driessche, J.; Bretagne, E.; Lotout, C.; Cogné, N. Late Variscan (315 Ma) subduction or deceptive zircon REE patterns and U-Pb dates from migmatite-hosted eclogites? (Montagne Noire, France). *J. Metamorph. Geol.* **2022**, *40*, 39–65. [CrossRef]
220. Franke, W. *The Mid-European Segment of the Variscides: Tectonostratigraphic Units, Terrane Boundaries and Plate Tectonic Evolution*; Geological Society Special Publications: London, UK, 2000; Volume 179, pp. 35–61. [CrossRef]
221. Medaris, L.G.; Beard, B.L.; Jelínek, E. Mantle-Derived, UHP Garnet Pyroxenite and Eclogite in the Moldanubian Gföhl Nappe, Bohemian Massif: A Geochemical Review, New P-T Determinations, and Tectonic Interpretation. *Int. Geol. Rev.* **2006**, *48*, 765–777. [CrossRef]
222. Kotková, J. High-pressure granulites of the Bohemian Massif: Recent advances and open questions. *J. Geosci.* **2007**, *52*, 45–71. [CrossRef]
223. Schulmann, K.; Lexa, O.; Štípská, P.; Racek, M.; Tajčmanová, L.; Konopásek, J.; Edel, J.B.; Peschler, A.; Lehmann, J. Vertical extrusion and horizontal channel flow of orogenic lower crust: Key exhumation mechanisms in large hot orogens? *J. Metamorph. Geol.* **2008**, *26*, 273–297. [CrossRef]
224. Schulmann, K.; Konopásek, J.; Janoušek, V.; Lexa, O.; Lardeaux, J.M.; Edel, J.B.; Štípská, P.; Ulrich, S. An Andean type Palaeozoic convergence in the Bohemian Massif. *Comptes Rendus Geosci.* **2009**, *341*, 266–286. [CrossRef]
225. Lexa, O.; Schulmann, K.; Janoušek, V.; Štípská, P.; Guy, A.; Racek, M. Heat sources and trigger mechanisms of exhumation of HP granulites in Variscan orogenic root. *J. Metamorph. Geol.* **2011**, *29*, 79–102. [CrossRef]
226. Chopin, F.; Schulmann, K.; Štípská, P.; Martelat, J.; Pitra, P.; Lexa, O.; Petri, B. Microstructural and metamorphic evolution of a high-pressure granitic orthogneiss during continental subduction (Orlica-Śnieżnik dome, Bohemian Massif). *J. Metamorph. Geol.* **2012**, *30*, 347–376. [CrossRef]
227. Faryad, S.W.; Jedlicka, R.; Ettinger, K. Subduction of lithospheric upper mantle recorded by solid phase inclusions and compositional zoning in garnet: Example from the Bohemian Massif. *Gondwana Res.* **2013**, *23*, 944–955. [CrossRef]

228. Timmermann, H.; Stedrá, V.; Gerdes, A.; Noble, S.R.; Parrish, R.R.; Dörr, W. The Problem of Dating High-pressure Metamorphism: A U-Pb Isotope and Geochemical Study on Eclogites and Related Rocks of the Marianske Lazne Complex, Czech Republic. *J. Petrol.* **2004**, *45*, 1311–1338. [CrossRef]
229. Konopásek, J.; Schulmann, K. Contrasting Early Carboniferous field geotherms: Evidence for accretion of a thickened orogenic root and subducted Saxothuringian crust (Central European Variscides). *J. Geol. Soc.* **2005**, *162*, 463–470. [CrossRef]
230. Linnemann, U.; Romer, R.L. *Pre-Mesozoic Geology of Saxo-Thuringia*; Schweizerbart Science Publishers: Stuttgart, Germany, 2010.
231. Faryad, S.W. High-pressure polymetamorphic garnet growth in eclogites from the Mariánskéázně Complex (Bohemian Massif). *Eur. J. Mineral.* **2012**, *24*, 483–497. [CrossRef]
232. Schaltegger, U.; Fanning, C.M.; Günther, D.; Maurin, J.C.; Schulmann, K.; Gebauer, D. Growth, annealing and recrystallization of zircon and preservation of monazite in high-grade metamorphism: Conventional and in-situ U-Pb isotope, cathodoluminescence and microchemical evidence. *Contrib. Mineral. Petrol.* **1999**, *134*, 186–201. [CrossRef]
233. Gayk, T.; Kleinschrodt, R. Hot contacts of garnet peridotites in middle/upper crustal levels: New constraints on the nature of the late Variscan high-T/low-P event in the Moldanubian (Central Vosges/NE France). *J. Metamorph. Geol.* **2000**, *18*, 293–305. [CrossRef]
234. Kalt, A.; Altherr, R.; Hanel, M. The Variscan basement of the Schwarzwald. *Eur. J. Mineral.* **2000**, *12*, 1–43.
235. Chen, F.; Todt, W.; Hann, H.P. Zircon and Garnet Geochronology of Eclogites from the Moldanubian Zone of the Black Forest, Germany. *J. Geol.* **2003**, *111*, 207–222. [CrossRef]
236. Marschall, H.R.; Kalt, A.; Hanel, M. P-T Evolution of a Variscan Lower-Crustal Segment: A Study of Granulites from the Schwarzwald, Germany. *J. Petrol.* **2003**, *44*, 227–253. [CrossRef]
237. Kober, B.; Kalt, A.; Hanel, M.; Pidgeon, R.T. SHRIMP dating of zircons from high-grade metasediments of the Schwarzwald/SW-Germany and implications for the evolution of the Moldanubian basement. *Contrib. Mineral. Petrol.* **2004**, *147*, 330–345. [CrossRef]
238. Edel, J.B.; Schulmann, K. Geophysical constraints and model of the "Saxothuringian and Rhenohercynian subductions—Magmatic arc system" in NE France and SW Germany. *Bull. Soc. Geol. Fr.* **2009**, *180*, 545–558. [CrossRef]
239. Altherr, R.; Holl, A.; Hegner, E.; Langer, C.; Kreuzer, H. High-potassium, calc-alkaline I-type plutonism in the European Variscides: Northern Vosges (France) and northern Schwarzwald (Germany). *Lithos* **2000**, *50*, 51–73. [CrossRef]
240. Faure, M.; Monié, P.; Pin, C.; Maluski, H.; Leloix, C. Late Visean thermal event in the northern part of the French Massif Central: New 40Ar/39Ar and Rb-Sr isotopic constraints on the Hercynian syn-orogenic extension. *Int. J. Earth Sci.* **2002**, *91*, 53–75. [CrossRef]
241. Edel, J.B.; Schulmann, K.; Skrzypek, E.; Cocherie, A. Tectonic evolution of the European Variscan belt constrained by palaeomagnetic, structural and anisotropy of magnetic susceptibility data from the Northern Vosges magmatic arc (eastern France). *J. Geol. Soc.* **2013**, *170*, 785–804. [CrossRef]
242. Skrzypek, E.; Tabaud, A.S.; Edel, J.B.; Schulmann, K.; Cocherie, A.; Guerrot, C.; Rossi, P. The significance of Late Devonian ophiolites in the Variscan orogen: A record from the Vosges Klippen Belt. *Int. J. Earth Sci.* **2012**, *101*, 951–972. [CrossRef]
243. Skrzypek, E.; Schulmann, K.; Tabaud, A.S.; Edel, J.B. *Palaeozoic Evolution of the Variscan Vosges Mountains*; Geological Society Special Publications: London, UK, 2014; Volume 405, pp. 45–75. [CrossRef]
244. Lardeaux, J.M.; Schulmann, K.; Faure, M.; Janoušek, V.; Lexa, O.; Skrzypek, E.; Edel, J.B.; Štípská, P. *The Moldanubian Zone in the French Massif Central, Vosges/Schwarzwald and Bohemian Massif Revisited: Differences and Similarities*; Geological Society Special Publications: London, UK, 2014; Volume 405, pp. 7–44. [CrossRef]
245. Ledru, P.; Courrioux, G.; Dallain, C.; Lardeaux, J.; Montel, J.; Vanderhaeghe, O.; Vitel, G. The Velay dome (French Massif Central): Melt generation and granite emplacement during orogenic evolution. *Tectonophysics* **2001**, *342*, 207–237. [CrossRef]
246. Faure, M.; Cocherie, A.; Mézème, E.B.; Charles, N.; Rossi, P. Middle Carboniferous crustal melting in the Variscan Belt: New insights from U-Th-Pbtot. monazite and U-Pb zircon ages of the Montagne Noire Axial Zone (southern French Massif Central). *Gondwana Res.* **2010**, *18*, 653–673. [CrossRef]
247. Franke, W.; Doublier, M.P.; Klama, K.; Potel, S.; Wemmer, K. Hot metamorphic core complex in a cold foreland. *Int. J. Earth Sci.* **2011**, *100*, 753–785. [CrossRef]
248. Faure, M.; Cocherie, A.; Gaché, J.; Esnault, C.; Guerrot, C.; Rossi, P.; Wei, L.; Qiuli, L. *Middle Carboniferous Intracontinental Subduction in the Outer Zone of the Variscan Belt (Montagne Noire Axial Zone, French Massif Central): Multimethod Geochronological Approach of Polyphase Metamorphism*; Geological Society Special Publications: London, UK, 2014; Volume 405, pp. 289–311. [CrossRef]
249. Bellot, J.P.; Triboulet, C.; Laverne, C.; Bronner, G. Evidence for two burial/exhumation stages during the evolution of the Variscan belt, as exemplified by P-T-t-d paths of metabasites in distinct allochthonous units of the Maures massif (SE France). *Int. J. Earth Sci.* **2003**, *92*, 7–26. [CrossRef]
250. Palmeri, R.; Fanning, M.; Franceschelli, M.; Memmi, I.; Ricci, C.A. SHRIMP dating of zircons in eclogite from the Variscan basement in north-eastern Sardinia (Italy). *Neues Jahrb. Mineral.—Monatshefte* **2004**, *2004*, 275–288. [CrossRef]
251. Giacomini, F.; Bomparola, R.M.; Ghezzo, C. Petrology and geochronology of metabasites with eclogite facies relics from NE Sardinia: Constraints for the Palaeozoic evolution of Southern Europe. *Lithos* **2005**, *82*, 221–248. [CrossRef]

252. Giacomini, F.; Dallai, L.; Carminati, E.; Tiepolo, M.; Ghezzo, C. Exhumation of a Variscan orogenic complex: Insights into the composite granulitic–Amphibolitic metamorphic basement of south-east Corsica (France). *J. Metamorph. Geol.* **2008**, *26*, 403–436. [CrossRef]
253. Franceschelli, M.; Puxeddu, M.; Cruciani, G.; Utzeri, D. Metabasites with eclogite facies relics from Variscides in Sardinia, Italy: A review. *Int. J. Earth Sci.* **2007**, *96*, 795–815. [CrossRef]
254. Corsini, M.; Rolland, Y. Late evolution of the southern European Variscan belt: Exhumation of the lower crust in a context of oblique convergence. *Comptes Rendus Geosci.* **2009**, *341*, 214–223. [CrossRef]
255. Rossi, P.; Oggiano, G.; Cocherie, A. A restored section of the "southern Variscan realm" across the Corsica–Sardinia microcontinent. *Comptes Rendus Geosci.* **2009**, *341*, 224–238. [CrossRef]
256. Morillon, A.C.; Féraud, G.; Sosson, M.; Ruffet, G.; Crevola, G.; Lerouge, G. Diachronous cooling on both sides of a major strike slip fault in the Variscan Maures Massif (south-east France), as deduced from a detailed 40Ar/39Ar study. *Tectonophysics* **2000**, *321*, 103–126. [CrossRef]
257. Conti, P.; Carmignani, L.; Funedda, A. Change of nappe transport direction during the Variscan collisional evolution of central-southern Sardinia (Italy). *Tectonophysics* **2001**, *332*, 255–273. [CrossRef]
258. Bellot, J.P. The Palaeozoic evolution of the Maures massif (France) and its potential correlation with others areas of the Variscan belt: A review. *J. Virtual Explor.* **2005**, *19*, 4. [CrossRef]
259. Elter, F.M.; Pandeli, E. Structural-Metamorphic Correlations Between Three Variscan Segments In Southern Europe: Maures Massif (France), Corsica(France)-Sardinia(Italy), And Northern Appennines (Italy). *J. Virtual Explor.* **2005**, *19*, 1. [CrossRef]
260. Carosi, R.; Montomoli, C.; Tiepolo, M.; Frassi, C. Geochronological constraints on post-collisional shear zones in the Variscides of Sardinia (Italy). *Terra Nova* **2012**, *24*, 42–51. [CrossRef]
261. Medaris, G.; Jelínek, E.; Beard, B.; Valley, J.; Spicuzza, M.; Strnad, L. Garnet pyroxenite in the Biskupice peridotite, Bohemian Massif: Anatomy of a Variscan high-pressure cumulate. *J. Geosci.* **2013**, *58*, 3–19. [CrossRef]
262. Maierová, P.; Lexa, O.; Schulmann, K.; Štípská, P. Contrasting tectono-metamorphic evolution of orogenic lower crust in the Bohemian Massif: A numerical model. *Gondwana Res.* **2014**, *25*, 509–521. [CrossRef]
263. Štípská, P.; Powell, R.; Hacker, B.R.; Holder, R.; Kylander-Clark, A.R.C. Uncoupled U/Pb and REE response in zircon during the transformation of eclogite to mafic and intermediate granulite (Blanský les, Bohemian Massif). *J. Metamorph. Geol.* **2016**, *34*, 551–572. [CrossRef]
264. Collett, S.; Štípská, P.; Schulmann, K.; Peřestý, V.; Soldner, J.; Anczkiewicz, R.; Lexa, O.; Kylander-Clark, A. Combined Lu-Hf and Sm-Nd geochronology of the Mariánské ázně Complex: New constraints on the timing of eclogite- and granulite-facies metamorphism. *Lithos* **2018**, *304–307*, 74–94. [CrossRef]
265. Maierová, P.; Schulmann, K.; Štípská, P.; Gerya, T.; Lexa, O. Trans-lithospheric diapirism explains the presence of ultra-high pressure rocks in the European Variscides. *Commun. Earth Environ.* **2021**, *2*, 56. [CrossRef]
266. Collett, S.; Schulmann, K.; Deiller, P.; Štípská, P.; Peřestý, V.; Ulrich, M.; Jiang, Y.; de Hoÿm de Marien, L.; Míková, J. Reconstruction of the mid-Devonian HP-HT metamorphic event in the Bohemian Massif (European Variscan belt). *Geosci. Front.* **2022**, *13*, 101374. [CrossRef]
267. Collett, S.; Schulmann, K.; Štípská, P.; Míková, J. Chronological and geochemical constraints on the pre-variscan tectonic history of the Erzgebirge, Saxothuringian Zone. *Gondwana Res.* **2020**, *79*, 27–48. [CrossRef]
268. Altherr, R. Retrograded garnet peridotites from Col des Bagenelles and Crébimont in the Variscan Vosges Mountains (NE France). *Contrib. Mineral. Petrol.* **2021**, *176*, 53. [CrossRef]
269. Tabaud, A.S.; Janoušek, V.; Skrzypek, E.; Schulmann, K.; Rossi, P.; Whitechurch, H.; Guerrot, C.; Paquette, J.L. Chronology, petrogenesis and heat sources for successive Carboniferous magmatic events in the Southern–Central Variscan Vosges Mts (NE France). *J. Geol. Soc.* **2014**, *172*, 87–102. [CrossRef]
270. Benmammar, A.; Berger, J.; Triantafyllou, A.; Duchene, S.; Bendaoud, A.; Baele, J.M.; Bruguier, O.; Diot, H. Pressure-temperature conditions and significance of Upper Devonian eclogite and amphibolite facies metamorphisms in southern French Massif central. *BSGF—Earth Sci. Bull.* **2020**, *191*, 28. [CrossRef]
271. de Hoÿm de Marien, L.; Pitra, P.; Poujol, M.; Cogné, N.; Cagnard, F.; Le Bayon, B. Complex geochronological record of an emblematic Variscan eclogite (Haut-Allier, French Massif Central). *J. Metamorph. Geol.* **2023**, *41*, 1–29. [CrossRef]
272. Whitney, D.L.; Hamelin, C.; Teyssier, C.; Raia, N.H.; Korchinski, M.S.; Seaton, N.C.A.; Bagley, B.C.; von der Handt, A.; Roger, F.; Rey, P.F. Deep crustal source of gneiss dome revealed by eclogite in migmatite (Montagne Noire, French Massif Central). *J. Metamorph. Geol.* **2020**, *38*, 297–327. [CrossRef]
273. Cruciani, G.; Franceschelli, M.; Groppo, C. P-T evolution of eclogite-facies metabasite from NE Sardinia, Italy: Insights into the prograde evolution of Variscan eclogites. *Lithos* **2011**, *121*, 135–150. [CrossRef]
274. Schneider, J.; Corsini, M.; Reverso-Peila, A.; Lardeaux, J.M. *Thermal and Mechanical Evolution of an Orogenic Wedge During Variscan Collision: An Example in the Maures–Tanneron Massif (SE France)*; Geological Society Special Publications: London, UK, 2014; Volume 405, pp. 313–331. [CrossRef]
275. Cruciani, G.; Franceschelli, M.; Groppo, C.; Oggiano, G.; Spano, M.E. Re-equilibration history and P-T path of eclogites from Variscan Sardinia, Italy: A case study from the medium-grade metamorphic complex. *Int. J. Earth Sci.* **2015**, *104*, 797–814. [CrossRef]

276. Cruciani, G.; Franceschelli, M.; Carosi, R.; Montomoli, C. P-T path from garnet zoning in pelitic schist from NE Sardinia, Italy: Further constraints on the metamorphic and tectonic evolution of the north Sardinia Variscan belt. *Lithos* **2022**, *428–429*, 106836. [CrossRef]
277. Cruciani, G.; Dulcetta, L.; Franceschelli, M.; Frassi, C.; Musumeci, G. Hot metamorphic complex in the Foreland Zone of the Variscan chain: Insights from the Monte Filau orthogneiss (SW Sardinia), Italy. *Ital. J. Geosci.* **2022**, *141*, 385–399. [CrossRef]
278. Jouffray, F.; Lardeaux, J.M.; Tabaud, A.S.; Corsini, M.; Schneider, J. Deciphering the nature and age of the protoliths and peak P-T conditions in retrogressed mafic eclogites from the Maures-Tannneron Massif (SE France) and implications for the southern European Variscides. *BSGF—Earth Sci. Bull.* **2023**, *194*, 10. [CrossRef]
279. Edel, J.B.; Casini, L.; Oggiano, G.; Rossi, P.; Schulmann, K. *Early Permian 90° Clockwise Rotation of the Maures-Estérel-Corsica-Sardinia Block Confirmed by New Palaeomagnetic Data and Followed by a Triassic 60° Clockwise Rotation*; Geological Society Special Publications: London, UK, 2014; Volume 405, pp. 333–361. [CrossRef]
280. Edel, J.B.; Schulmann, K.; Lexa, O.; Lardeaux, J.M. Late Palaeozoic palaeomagnetic and tectonic constraints for amalgamation of Pangea supercontinent in the European Variscan belt. *Earth-Sci. Rev.* **2018**, *177*, 589–612. [CrossRef]
281. Oliot, E.; Melleton, J.; Schneider, J.; Corsini, M.; Gardien, V.; Rolland, Y. Variscan crustal thickening in the Maures-Tanneron massif (South Variscan belt, France): New in situ monazite U-Th-Pb chemical dating of high-grade rocks. *Bull. Soc. Fr.* **2015**, *186*, 145–169. [CrossRef]
282. Gerbault, M.; Schneider, J.; Reverso-Peila, A.; Corsini, M. Crustal exhumation during ongoing compression in the Variscan Maures-Tanneron Massif, France-Geological and thermo-mechanical aspects. *Tectonophysics* **2018**, *746*, 439–458. [CrossRef]
283. Rubatto, D. Dating of Pre-Alpine magmatism, Jurassic Ophiolites and Alpine Subductions in the Western Alps. Ph.D. Thesis, ETH—Zurich, Zurich, Switzerland, 1998.
284. Vho, A.; Rubatto, D.; Lanari, P.; Regis, D. The evolution of the Sesia Zone (Western Alps) from Carboniferous to Cretaceous: Insights from zircon and allanite geochronology. *Swiss J. Geosci.* **2020**, *113*, 24. [CrossRef]
285. Delleani, F.; Rebay, G.; Zucali, M.; Tiepolo, M.; Spalla, M.I. Insights on Variscan geodynamics from the structural and geochemical characterization of a Devonian-Carboniferous gabbro from the Austroalpine Domain (Western Alps). *Ofioliti* **2018**, *43*, 23–29. [CrossRef]
286. Sloman, L.E. Triassic shoshonites from the Dolo- mites, Northern Italy: Alkaline arc rocks in a strike- slip setting. *J. Geophys. Res.* **1989**, *94*, 4655–4666. [CrossRef]
287. Lustrino, M.; Abbas, H.; Agostini, S.; Caggiati, M.; Carminati, E.; Gianolla, P. Origin of Triassic magmatism of the Southern Alps (Italy): Constraints from geochemistry and Sr-Nd-Pb isotopic ratios. *Gondwana Res.* **2019**, *75*, 218–238. [CrossRef]
288. Cocks, L.; Torsvik, T. Earth geography from 500 to 400 million years ago: A faunal and palaeomagnetic review. *J. Geol. Soc.* **2002**, *159*, 631–644. [CrossRef]
289. Nance, R.D.; Gutiérrez-Alonso, G.; Keppie, J.D.; Linnemann, U.; Murphy, J.B.; Quesada, C.; Strachan, R.A.; Woodcock, N.H. Evolution of the Rheic Ocean. *Gondwana Res.* **2010**, *17*, 194–222. [CrossRef]
290. Linnemann, U.; Gerdes, A.; Drost, K.; Buschmann, B. The continuum between Cadomian orogenesis and opening of the Rheic Ocean: Constraints from LA-ICP-MS U-Pb zircon dating and analysis of plate-tectonic setting (Saxo-Thuringian zone, northeastern Bohemian Massif, Germany). In *The Evolution of the Rheic Ocean: From Avalonian-Cadomian Active Margin to Alleghenian-Variscan Collision*; Geological Society of America: Washington, DC, USA, 2007. [CrossRef]
291. Marotta, A.M.; Roda, M.; Conte, K.; Spalla, M.I. Thermo-mechanical numerical model of the transition from continental rifting to oceanic spreading: The case study of the Alpine Tethys. *Geol. Mag.* **2018**, *155*, 250–279. [CrossRef]
292. Furlong, K.P.; Chapman, D.S. Heat Flow, Heat Generation, and the Thermal State of the Lithosphere. *Annu. Rev. Earth Planet. Sci.* **2013**, *41*, 385–410. [CrossRef]
293. Doré, A.G.; Stewart, I.C. Similarities and differences in the tectonics of two passive margins: The Northeast Atlantic Margin and the Australian North West Shelf. In *The Sedimentary Basins of Western Australia 3*; Keep, M., Moss, S.J., Eds.; Petroleum Exploration Society of Australia (PESA): Beaumaris, VIC, Australia, 2002; pp. 89–117.